Evolutionary Biology
https://doi.org/10.1007/s11692-023-09613-4

RESEARCH ARTICLE

Geographic Drivers of Genetic and Plumage Color Diversity in the Blue-Crowned Manakin

Pedro Paulo[1,2] · Fernando Henrique Teófilo[1,2,14] · Carolina Bertuol[1,3,12] · Érico Polo[3] · Andre E. Moncrieff[4] · Lucas N. Bandeira[1,2] · Claudia Nuñez-Penichet[5] · Igor Yuri Fernandes[2] · Mariane Bosholn[1,2,6] · Arielli F. Machado[1,7] · Leilton Willians Luna[9,10] · Willian Thomaz Peçanha[8] · Aline Pessutti Rampini[1,2] · Shizuka Hashimoto[1,3] · Cleyssian Dias[9,10] · Juliana Araripe[9] · Alexandre Aleixo[10,11,15] · Péricles Sena do Rêgo[9] · Tomas Hrbek[3,12] · Izeni P. Farias[3,12] · A. Townsend Peterson[5] · Igor L. Kaefer[2,13] · Marina Anciães[1,2]

Received: 21 February 2021 / Accepted: 17 July 2023

Abstract

Investigating parallel roles of geography and environmental heterogeneity in diversification provides insights on how neutral and selective forces drive evolution of biological systems. Here, we investigate whether geographic and climatic distances explain either genetic or phenotypic variation in Blue-crowned Manakins (*Lepidothrix coronata*), a polychromatic bird species that is broadly distributed in the Neotropics. We tested the hypotheses of isolation by distance and environment through an integrative approach using genetic, colorimetric, geographic, and environmental data. Through structural equation modeling and multiple matrix regression with randomization statistics, we tested whether intraspecific genetic or phenotypic (plumage color) diversity is associated with variation in geographic and environmental distances among localities. Genetic and color diversity were not correlated: color variation was marginally associated with latitude; and genetic distances were explained by linear and least-cost geographic distances, conforming to predictions of isolation by distance and by environment. We suggest a combined effect of genetic drift and environmental heterogeneity in driving the genetic diversification at the regional scale, and adaptation to local environments operating in the diversification of adult male plumage coloration.

Keywords Color variation · Genetic structure · Least cost corridors · *Lepidothrix coronata* · Multiple matrix regression with randomization · Neutral drift

Introduction

Phenotypic variation may be the result of adaptive (Cadena et al., 2011) or neutral processes (Lee et al., 2016; Rojas et al., 2020), and can be related to the geographic distribution of a taxon (Amézquita et al., 2009), reflecting underlying genetic structure (Thom et al., 2018). The study of phenotypic variation can provide information on landscape discontinuities (Wang & Shaffer, 2008), ecological speciation (Seehausen et al., 2008), selective pressures (Boul et al., 2007), and adaptation to new environments (Benites et al., 2020). Therefore, investigating the role of these factors in nature can provide insights into processes underlying the evolutionary history of different taxa (Boul et al., 2007; Maia et al., 2017).

Many factors can reduce gene flow, promoting phenotypic differentiation and, ultimately, speciation because of geographic isolation (Wright, 1943) or ecological differentiation (Schluter, 2001). Processes underlying these patterns can include isolation by distance (hereafter IBD; Wright, 1943) or isolation by environment (hereafter IBE; Wang & Bradburd, 2014). IBD results from restrictions to gene flow posed by geographic distance in the absence of natural barriers (e.g., Cadena et al., 2011; Rojas et al., 2020), producing positive correlations between genetic or phenotypic divergence and geographic distances among localities. This relationship is the most common diversification mechanism observed and studied in nature (Ramírez-Barrera et al., 2019; Wright, 1943). In turn, IBE occurs when the gene flow is restricted by individual or population preferences for staying in an environment or by environmentally driven selection against dispersal among populations (Ramírez-Barrera et al., 2019;

Extended author information available on the last page of the article

Published online: 22 August 2023

Wang & Bradburd, 2014). Thus, environmental variation can be examined as a relationship between genetic or phenotypic divergence and environmental dissimilarity.

The passerine bird genus *Lepidothrix* (Bonaparte, 1854), with eight recognized species, is the most species-rich genus in the family Pipridae (Kirwan & Green, 2011; Snow, 2020; but see Moncrieff et al., 2022). Members of *Lepidothrix* are distinguished primarily based on plumage color on the crown, breast, and rump of adult males (Snow, 2020). Females have more uniform coloration (shades of light green; Snow, 2020). Despite being so phenotypically diverse, phylogenetic relationships in this genus have not been resolved fully (Dias et al., 2018; Leite et al., 2020; Moncrieff et al., 2022). *Lepidothrix coronata* (Spix, 1825), the Blue-crowned Manakin, is the most geographically diverse species in this genus, with eight recognized subspecies based on adult male plumage patterns (Kirwan & Green, 2011), constituting one of the most interesting cases of geographic variation in plumage coloration among manakins. Male body feathers vary from yellow and green to black, and crown feathers vary from purplish-blue to sky-blue (Anciães et al., 2009; Cheviron et al., 2005; Kirwan & Green, 2011). Based on the color variation of their body plumage, the subspecies of *L. coronata* can be divided into two main groups: the coronata group (*L. c. coronata*, *L. c. carbonata*, *L. c. caquetae*, *L. c. minuscula*, *L. c. velutina*) in which adult males have black plumage, distributed in Costa Rica, Panama, Colombia, Ecuador, Peru, Venezuela, and Brazil (north of the Amazon River), and the *exquisita* group (*L. c. exquisita*, *L. c. caelestipileata*, *L. c. regalis*), in which adult males have mostly green body plumage and are distributed in central and southern Peru, Bolivia, and Brazil (south of the Amazon River). In the contact zone between the two groups, in southern Amazonia (in Peru and Brazil), males from some populations have intermediate body plumage phenotypes that were given their own names: "chloromelaena" (from Nova Olinda, on the left bank of the lower Purus River; Todd, 1925), "arimensis" (from Arima, on the right bank of the lower Purus River; Todd, 1925), "hoffmannsi" (from Tefé, upper Rio Solimões; Hellmayr, 1907), and "circumpicta" (near Yurimaguas, south of the Marañón River; Zimmer, 1936).

The Blue-crowned Manakin complex has a complicated evolutionary history. Cheviron et al. (2005) assessed congruence between subspecific taxonomy, plumage patterns, and phylogenetic relatedness among its populations. They found six well-supported clades (trans-Andean, Venezuela, Napo/Marañon, North Amazon, Central Peru, South Peru/Bolivia); however, only one subspecies was supported phylogenetically (*L. c. velutina*). This result suggests that current taxonomy does not reflect evolutionary patterns in the species. Possible causes of the discrepancies between taxonomy (and, consequently, adult male plumage coloration) and phylogeny may be the result of diverse processes, including introgression, incomplete lineage sorting, and local selective pressures on male plumage. More recently, Reis et al. (2020) using a multilocus approach and broader sampling, recovered three lineages east of the Andes: one bounded by the Japurá River (corresponding to the Venezuela clade of Cheviron et al., 2005), one north of the Amazon River (corresponding to the North Amazon and Napo/Marañon clade), and one south the Amazon River (corresponding to Central Peru and South Peru/Bolivia clade of Cheviron et al., 2005). They suggested that the lineage west of the Andes, the only showing congruence between plumage and phylogeny, was the first to diverge in the history of the complex. They also suggested that diversification in the Amazon Basin occurred mainly because Amazonian rivers create barriers to gene flow and promote diversification.

Despite multiple biogeographic studies of the Blue-crowned Manakin (Cheviron et al., 2005; Reis et al., 2020; Smith et al., 2014), no research has reflected on the role of environmental variation in the genetic and phenotypic divergence in the species. Furthermore, a knowledge gap exists regarding the relationship between genetic and phenotypic variation among populations covering the geographic range of the species. At least within the Purus-Madeira interfluvium, phenotypic variation among populations correlates with both geographic distances and vegetation structure (Teófilo et al., 2018). As such, environmental heterogeneity may be associated with phenotypic differentiation at broader geographic scales in the species range and may help to explain patterns of genetic divergence.

Here, we employed an integrative populational-level approach relating differences in genetic and coloration traits of Blue-crowned Manakins with geographic and climatic data across its geographic distribution. We sought to understand whether genetic or phenotypic variation is associated with variation in geographic distances and/or environmental differences among localities. We specifically tested whether (a) the geographic distance per se is related with genetic and phenotypic differentiation in the group (IBD); or (b) environmental heterogeneity influenced the group's diversification (IBE, Table 1).

Materials and Methods

Data Acquisition and Processing

Geographic Occurrence Data

We collected locality, genetic, and color data for Blue-crowned Manakins across their entire known geographic range (Fig. 1). The species is the most wide-ranging of the genus *Lepidothrix*, occurring from southern Central America

Table 1 Summary of hypotheses tested (Isolation by distance, Isolation by environment), predicted results, and interpretations according to plausible evolutionary processes explaining genetic and/or phenotypic diversification in Blue-crowned Manakins

Phenotypic variation		Genetic variation	Geographic pedictor	Environmental predictor	Hypothesis	Evolutionary mechanism
Yes	Or	Yes	Yes	No	Isolation by distance (IBD)	Genetic drift
Yes	Or	Yes	No	Yes	Isolation by environment (IBE)	Ecological diversification
Yes	And	Yes	No	Yes	Isolation by adaptation (IBA)*	Adaptation/selection

*IBA is considered a special case within IBE in which phenotypic and genetic variation are correlated and explained by the environment

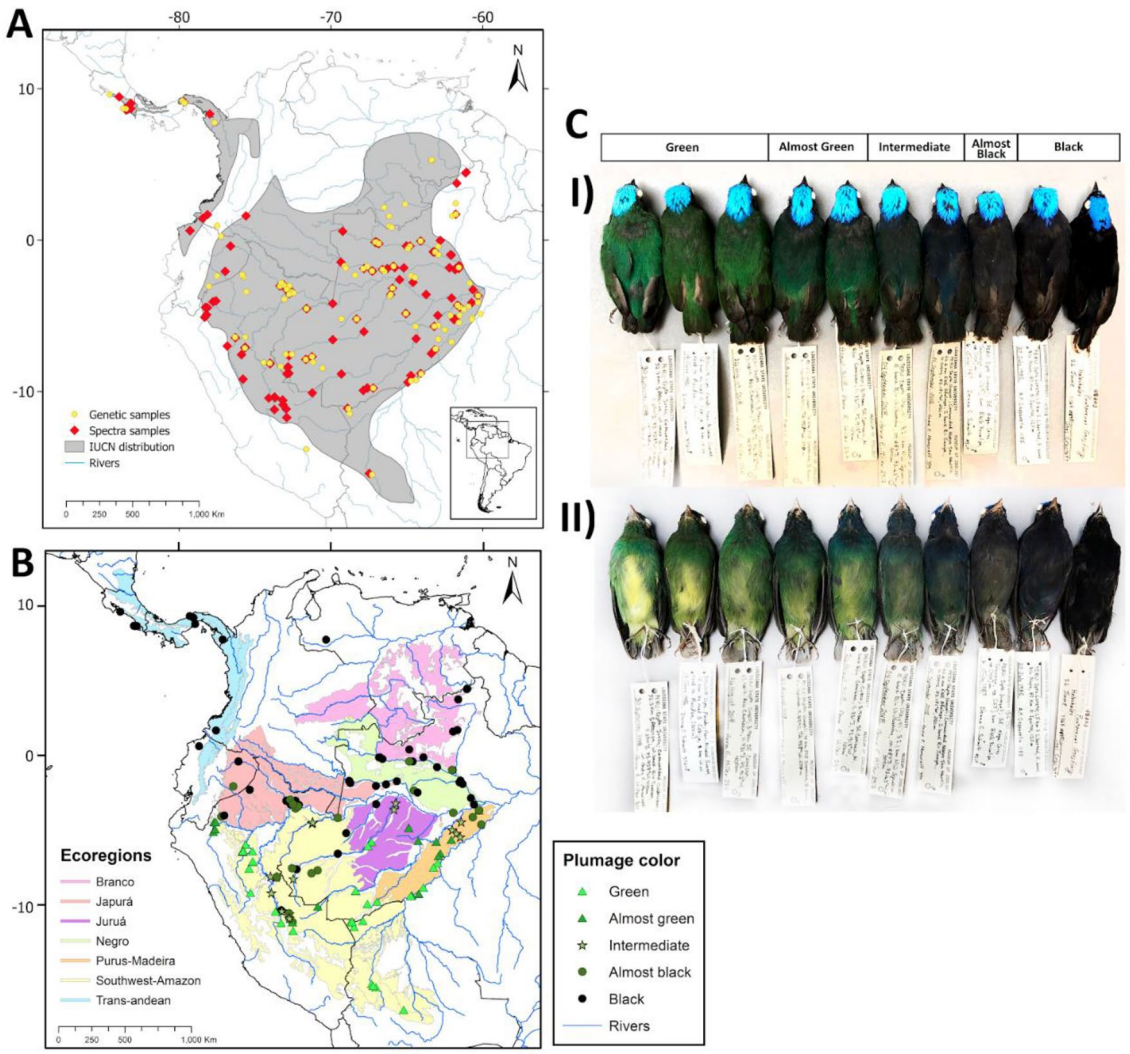

Fig. 1 **A** Geographic distribution of *Lepidothrix coronata* according to IUCN (in gray), localities with genetic samples used in this study (red diamonds), and spectra samples for male plumage coloration (yellow diamonds); **B** Categorical representation of the geographic variation in male plumage patterns in the species range represented by male plumage coloration sampled from museum specimens (MZUSP, LSUMNS, AMNH) exemplified in **C** dorsal (I) and ventral (II) views. Plumage patterns of adult males were classified according to the proportion of black and olive, yellow-green or green in the body: green when the back and breast are green, and the belly is yellow or green (1–3); almost green when only their throats and lores are blackish, with green or yellow-green belly and the back is green (4 and 5); intermediate when their back and breast are dark green or blackish and the belly is olive or green (6 and 7); almost black when only their lower underparts are dark olive and the back is black (8) and black for entirely black bodies (9 and 10). Plumage patterns were consistent among specimens from the same sampled location, excluding juveniles in transient plumage (Color figure online)

and western South America south to northern Bolivia (Kirwan & Green, 2011). The occurrence data included latitude–longitude information and the locations of sampling for specimens that yielded genetic and color data. We obtained these data from museum collections in Brazil (INPA, MPEG, MZUSP), Bolivia (MHNNKM), and the USA (LSUMNS, AMNH, USNM). We obtained additional occurrence data from the Global Biodiversity Information Facility (GBIF, https://www.gbif.org/), eBird (https://ebird.org/home), and Macaulay Library (https://www.macaulaylibrary.org/) online repositories. We cleaned the data by removing duplicates, missing coordinates, and coordinates falling outside of the species' known geographic distribution. We corrected, when possible, records with disagreement between specimen traits and the taxonomic identification attributed to them by the collectors, as well as records with inconsistencies in its latitude–longitude information (Cobos et al., 2018). After this cleaning process, we had 1205 occurrences of this species (from 2507 initial records), which were used to generate ecological niche models and least-cost corridors (see below).

We used the latitude and longitude values from each occurrence to build the geographic distance matrix. This step was performed only for coordinates from localities with both genetic and color information (134 localities, see below). We calculated pairwise distances among all localities using the package 'fossil' (Vavrek, 2011) in R v. 3.3.3 (R Development Core Team, 2020).

Environmental Data

We generated ecological niche models (ENM) based on 15 climatic variables for the period 1970–2000 from WorldClim database (https://www.worldclim.org/, Hijmans et al., 2005), at a spatial resolution of 2.5′ arc-minutes (~ 5 km^2) (Online Appendix S2). We excluded Bio08, Bio09, Bio18, and Bio19 because they combined temperature and precipitation information that leads to artifacts in the results (Escobar et al., 2014). The variables were cut using a mask (calibration area [M]; Soberón & Peterson, 2005) created with the ecoregions defined in Dinerstein et al. (2017) and the limits of the known geographical distribution of *L. coronata*, to approximate the areas accessible for the species over relevant periods of time (Barve et al., 2011). This step was done with the packages 'raster' (Hijmans et al., 2015), 'sp' (Pebesma et al., 2013), 'rgeos' (Bivand et al., 2017), 'rgdal' (Bivand et al., 2015), 'fields' (Furrer et al., 2009), 'shapefiles' (Stabler & Stabler, 2013), 'maptools' (Lewin-Koh et al., 2012), and 'maps' (Becker et al., 2021) in R v. 3.3.3 (R Development Core Team, 2020). From the 15 variables, we eliminated one from each pair of variables with a Pearson's correlation > 0.8. This procedure resulted in retention of six variables for analysis: annual mean temperature, mean diurnal range, temperature seasonality, mean temperature of coldest quarter, precipitation seasonality, and precipitation of driest quarter.

We ran ENMs using the package 'kuenm' (Cobos et al., 2019) in R v. 3.3.3 (R Development Core Team, 2020) and following Simões et al. (2020). Model calibration and parameter evaluation sets included the 1,205 clean occurrence records available for the species, and all combinations of the six selected environmental variables, 17 regularization multipliers (0.1, 0.2, 0.3, 0.4, 0.5, 0.6, 0.7, 0.8, 0.9, 1, 2, 3, 4, 5, 6, 8, 10), and 29 combinations of feature classes (combinations of linear (l), quadratic (q), product (p), threshold (t), and hinge (h) options), to select the best combinations (Cobos et al., 2019), using Maxent (Phillips et al., 2006, 2017). We ran partial Receiver Operating Characteristic (ROC) tests to evaluate model performance (Peterson et al., 2008), in tandem with omission rates < 5%, Anderson et al., 2003). We further filtered to retain only the models with values of Akaike Information Criterion corrected for small sample sizes (AICc; Warren & Seifert, 2011) with two units of the minimum, presented by any significant, low-omission candidate models. After model calibration, we selected the one model (of the 493 tested) conforming to all selection criteria and created the final model with the selected parameter settings (which were regularization multiplier = 0.3 and feature class = lqp) using all occurrences, 10,000 bootstrap replicates, and cloglog output (Phillips et al., 2017).

In addition to six variables selected from the ENM analysis, we explored environmental variables of topography and vegetation using elevation data derived from the Shuttle Radar Topography Mission (STRM) and the normalized difference vegetation (NDVI), derived from the Landsat 8 Surface Reflectance (Vermote et al., 2016), both downloaded via Copernicus (https://www.copernicus.eu/en). With that, our environmental dataset comprised eight variables in raster format. We extracted variable values from each pixel corresponding to all 134 locations using the package 'vegan' (Oksanen et al., 2013) in R v. 3.3.3 (R Development Core Team, 2020). We then standardized variable values through normalization to run a principal component analysis (PCA; Jolliffe, 1986) and used the first two PC axes to calculate pairwise environmental distances among localities using the package 'fossil' (Vavrek, 2011) in R v.3.3.3 (R Development Core Team, 2020). These procedures aimed at generating the environmental data for subsequent statistical analyses.

Least Cost Corridor Paths (LCCP)

We calculated least cost corridor paths (LCCP) to estimate connectivity among the species' current populations in geographic space, considering environmental suitability and differences (e.g., Nuñez-Penichet et al., 2019). This analysis allowed us to identify corridors of suitable habitats that may be used for individual movements through

the landscape and to predict potential current gene flow routes among populations (Chan et al., 2011). All data used for creating the LCCPs were from the current period, so the estimated potential corridors are not considering environmental connectivity of barriers present in the past (Warren, 2012; Warren et al., 2008). In this analysis, we only included geographic information from occurrence records (i.e., disregarding haplotype genetic data), to provide an estimate independent from the genetic data to be compared to the genetic and coloration distance matrices (see below).

We created a friction layer to calculate the LCCPs (with values from 0 to 10) by inverting the values of the species suitability map obtained from the ENM (range 0–1), so that areas with greater suitability presented lower resistance to displacement. For this analysis, we spatially thinned the 1205 occurrences by removing all occurrences that were closer than 5 km to another occurrence record, obtaining 88 points. This step was done in the package 'spThin' (Aiello-Lammens et al., 2015) in R v. 3.3.3 (R Development Core Team, 2020). Using the friction layer and the species occurrence records (88 records after spatial thinning), we estimated likely corridors used for movement among its populations. We also generated potential corridors with the friction layer and five distinct sets of random points, each with the same number of points as the used species occurrences (n = 88) that we generated at random within the suitable area identified in the ENM analyses. This analysis was done to explore potential movement routes based on the climatic niche models instead of actual records. The LCCPs obtained using the five sets of random points were summed and the corridors with the highest values of connectivity were considered the more likely routes favoring gene flow among populations. These procedures were performed using the SDMtoolbox 2.0 extension (Brown et al., 2017) of ArcGIS 10.5.1.

To generate the least environmental cost distance matrix, we created a transition object using the friction layer used for the LCCPs using pixel-by-pixel mean and an 8-way direction Moore neighborhood consisting of all pixels surrounding the target pixel (van Etten, 2017). We then corrected the transition object for longer values of diagonal connections as well as those closer to the equator using the function 'geoGorrection' and calculated the least environmental cost distance between points using the function 'costDistance' in package 'gdistance' (van Etten, 2017) in R v. 3.3.3 (R Development Core Team, 2020). These procedures generated the least-cost distances for subsequent statistical analyses, calculating the cost distance between the cells using the values of the transition matrix through Dijkstra's algorithm that considers the Euclidean distance.

Genetic Dataset

We obtained mitochondrial DNA (mtDNA) fragments of the Cytochrome Oxidase subunit I (*COI*), Cytochrome b (*CYTB*), partial NADH dehydrogenase 2 (*ND2*), and the entire NADH dehydrogenase 3 (*ND3*) genes for 112 individuals, plus 159 previously published sequences including mtDNA (*CYTB*, *ND2*, *ND3*) and nuclear DNA (nuDNA) fragments of Myoglobin (*MYO*), Glyceraldehyde-3-phosphate dehydrogenase (*G3PDH*), and Intron 5 of the beta fibrinogen (*FIB5*) obtained from GenBank (https://www.ncbi.nlm.nih.gov/genbank/). For this study, a total of 350 individuals from 134 localities were analyzed (Table S1). Sequences of *L. iris*, *L. serena*, and *L. coeruleocapilla* were used as outgroups in our phylogenetic analyses.

We extracted total DNA from muscle tissue using the 2% CTAB protocol (Doyle & Doyle, 1987). We amplified *COI* with the M13-tailed primers BirdF1 and BirdR1 (Ivanova et al., 2007), *ND2* with primers L5215 and H5578 (Hackett, 1996), *ND3* with primers L10755 and H11151 (Chesser, 1999), and *CYTB* with primers LepF2 LepR2, developed for this study (Table S3). We purified the PCR products with ExoSAP (Werle et al., 1994). We sequenced following the manufacturer's recommended protocol for BigDye Sequencing Kit (Applied Biosystems), but then precipitated with a 100% ethanol/125 mM EDTA solution, re-suspended in Hi-Di formamide, and then injected into an ABI 3500 automated sequencer (Applied Biosystems). We assembled, edited, aligned, and trimmed sequences using the software Geneious v8.1.8; we aligned sequences using the MUSCLE (Edgar, 2004) plugin in Geneious v8.1.8, and confirmed by eye.

While our statistical approach does not rely on the phylogenetic structure within the species, we provide the phylogeographic context of our sampling and analytical framework for possible bias detection from unrecognized genetic variation and systematic validation with previous studies. As such, we investigated population structure within *L. coronata* in Bayesian Analysis of Population Structure (BAPS), which estimates the K value that best explains the distribution of the individual samples into different genetic clusters. For this, nucleotide frequencies for DNA sequence data and the number of genetically diverged groups in the population were treated as random variables. We used the mtDNA sequences while considering linkage between polymorphic sites across all loci and allowed different maximum numbers of K in multiple runs, following recommendations from the manual in BAPS, version 6.0 (Corander et al., 2013; Tang et al., 2009).

We then considered two approaches for phylogenetic inferences: (1) based on a Bayesian phylogenetic tree generated from the concatenated individual sequences in the BEAST 2 program (Bouckaert et al., 2014), and (2) based on

species tree hypotheses from groups delimited with BAPS, using StarBeast2 (Bouckaert et al., 2014). We considered these two approaches because differences in the number of samples and loci with intronic (nuDNA) available relative to coding (mtDNA) loci could generate different tree topologies, and each method presents advantages in dealing with those complicating factors. We used PartitionFinder2 (Lanfear et al., 2017) to obtain the best partition model, as well as the best evolutionary model for each partition and tree. We considered each intronic (nuDNA) and coding (mtDNA) marker as one partition. For the BEAST tree, we split each coding marker in three. This split was done according to the base pair position in codons, resulting in 15 distinct initial partitions for the concatenated dataset. This process was done using the function 'rcluster' of this program. For the BEAST tree, we used the K80 + I + G (*MYO2*, *FIB5*, *G3PDH*), HKY + G + X (*ND2*_a, *COI*_c, *ND3*_b, *CYTB*_b), GTR + G + X (*ND3*_c, *CYTB*_c, *ND2*_b, *COI*_a), HKY + I + X (*ND2*_c), and K80 + I + G (*COI*_b, *ND3*_a, *CYTB*_a), whereas for the StarBeast2 tree we used the HKY + I + G + X evolutionary model for both nuDNA and mtDNA markers, and selected evolutionary models in Greedy for both trees (Lanfear et al., 2012). We then generated trees for separate loci according to the partitions from PartitionFinder2 and linking topologies and clocks fixed at a rate of 0.0105 nucleotides/lineage/Myr for cytb, following Weir and Schluter (2008) and estimated for the other mtDNA and nuDNA markers.

Finally, we estimated evolutionary relationships between haplotypes for each dataset (i.e. mitochondrial and nuclear) using the median-joining method implemented in Network v10.0 (http://www.fluxus-engineering.com). The regions for the haplotype network were defined using the ecoregion map from Dinerstein et al. (2017): Branco (including Japurá-Solimões-Negro moist forests and Guianan Piedmont moist forests), Japurá (including the Solimões-Japurá moist forest and Napo moist forests), Purus-Madeira moist forest, Southwest Amazonia (including the Bolivian Yungas, Central Andean Puna and Southwest Amazonia moist forests), Negro (including Japurá-Solimões-Negro moist forests), Trans-Andean (including Northwest Andean montane forests, Chocó-Darien moist forests, Isthmian-Atlantic moist forests, and Isthmian-Pacific moist forests), and Juruá (including Juruá-Purus moist forests), to convey environmental and historical information to the network. For the nuclear dataset, we used PHASE (Stephens et al., 2001) to reconstruct haplotypes for heterozygous individual loci from population data. To do so, we tested for recombination using phytes implemented in SplitsTree (Huson & Bryant, 2006) and found no evidence for recombination between segregating sites within loci, and accepted the best haplotype guesses, regardless of uncertainty, after 10 independent runs with 10,000 Markov Chain steps each and 1000 burn-in steps. Tajima D (1989) and Fu (1997) tests detect aspects of the demographic history of Blue-crowned Manakins such as previous population growth, and summarize diversity index, such as the number of variable sites (S), number of haplotypes (N_H), haplotype diversity (h), nucleotide diversity (π), and average number of nucleotide differences (k), identified computationally using the software DnaSP v5.10 (Librado & Rozas, 2009) and Arlequin v3.5 (Excoffier & Lischer, 2010). For more details see Appendix S3 and Table S4.

Because genetic distances among localities are generally not affected by differences in inter-node relationships, we generated genetic distances based only on the Bayesian phylogenetic tree obtained by the concatenated dataset. We ran a principal component analysis (PCA) using the software Jalview 2 (Waterhouse et al., 2009) for input in subsequent statistical analyses, either directly from the PCA output or the genetic distance matrix obtained from it. PCA is one of the most widely used methods to summarize population structure and genetic distance, allowing for the reduction of complexity in genetic data while maintaining covariance (Patterson et al., 2006). We fixed the clock to one in the BEAST tree, using a coalescent prior, and we ran 100 million steps in the Markov chain Monte Carlo, discarding the first 35 million steps necessary for obtaining ESS values of at least 200 for all parameters. We sampled BEAST trees every 10 thousand steps, obtaining at the end 6501 posterior trees, and then generated the genetic distance matrix by incorporating posterior uncertainties to distances obtained from the BEAST tree, using the function 'cophenetic.phylo' from the R package 'ape' (Paradis & Schliep, 2019). We then calculated one matrix for every 6501 posterior trees and averaged its values to represent the genetic distance matrix.

Coloration Dataset

We photographed specimens and classified color patterns of their body plumages into five categories, to include the variation described for the species (del Hoyo et al., 2004; Kirwan & Green, 2011) including, from lighter to darker: green, almost green, intermediate, almost black, and black. As such we could map the geographic variation in male body plumage patterns as they are usually described in categories. We then measured plumage coloration of Blue-crowned Manakins with a spectrophotometer from 259 adult male specimens of *L. coronata*, from the same 134 locations mentioned above, covering much of the variation in male plumage visible to humans (considering the body patterns ascribed above and crown color).

We obtained plumage reflectance spectra for 10 plumage patches for each specimen (back, belly, breast, crown, crown edge, rump, tail, throat, upper wing or wing1, and lower wing or wing2; Online Appendix S4), using a USB2000 spectrophotometer (Ocean Optics) with an Ocean Optics

PX-2 pulsed xenon light source, connected to a bifurcated fiber-optic probe. Measurements followed standard procedures (Eaton, 2005) to record reflectance for the wavelength interval within the avian visual spectrum, from 300 to 700 nm (Goldsmith, 1990). We visualized and manipulated the reflectance spectra in the R package 'PAVO' (Maia et al., 2019) and estimated variation of coloration pattern for the species using 23 metrics (Table S5) summarizing hue (peak location), saturation (purity), and brightness (intensity), for all plumage regions considering the tetrachromatic visual system of birds (Goldsmith, 1990) and setting the V-type eye typical of manakins (Ödeen & Håstad, 2013).

We ran two Principal Component Analyses (PCA; Jolliffe, 1986) based on Euclidean distances on raw data, with extracted metrics (Online Appendix S4.b; Tables S5–S7; Fig. S2) to summarize variation for input into subsequent analyses. We calculated the coloration distance matrix as the average pairwise difference in units of jnd (just noticeable differences), setting 2 jnds as threshold for visual perception of differences (Eaton, 2005; Osorio, 1996; Vorobyev et al., 2001), with the package PAVO (Maia et al., 2019) in R v.3.3.3 (R Development Core Team, 2020). To do this step, we estimated the color distance in jnds for each plumage region from each pair of individuals from all pairwise comparisons between locations (i.e., one individual from each) and averaged values among plumage regions (Fig. S4).

Statistical Analyses

We performed a structural equation modeling (SEM) analysis using the *'lavaan'* package (Rosseel, 2012) in R (R Development Core Team, 2020) after obtaining the PCA1 for each dataset and latitude–longitude data. We used the PCA as an input to the SEM so that the variables are reduced because of the autocorrelation that exists between many variables of the same category (e.g. climate, colorimetric), allowing the observation of data variation as a whole. We chose to use PC1 because it normally concentrates the largest volume of variation in relation to the other PCs in the PCA analysis. However, the use of more PCs in the SEM analysis would imply increasing the complexity of the proposed model, in addition to confusing the analysis, since in several cases the variables of PC1 are correlated with those of PC2. SEMs investigates the relationships between latent and observed variables through regressions between models, as well as their covariations, allowing simultaneous assessment of combined influences of multiple factors (Rosseel, 2012).

To address the effect of geographic distance in our datasets, we used the distance matrices to implement multiple matrix regression with randomization (MMRR) analyzes in R, following Wang (2013), to test how linear and least-cost geographic distances relate to genetic and coloration differences between locations. This analysis incorporates multiple regressions separately for each pair of distance matrices considered in the study, and the output is in the form of a multiple regression equation (Wang, 2013). As such, multiple regression analysis is used to estimate how genetic or phenotypic distance (response variable) is affected by changes in linear or least cost geographic and environmental distances (predictor variables), estimating the overall fit of the model (R^2 = coefficient of determination), and the significance of each variable (p-values, P). We performed analyses considering a single predictor at a time, either geographic or environmental or least cost distances.

Results

Ecological Niche Models and Least-Cost Corridors

The variable mean temperature of the coldest quarter (Bio12) was the one that contributed the most to the selected ecological niche model (32%, Table S2). The suitable areas for *L. coronata* were widespread across the calibration area, with the highest values of suitability found in Costa Rica, Panama, in both sides of the Colombian Andes, and in Brazil, within the limits of Napo endemism area (sensu Cracraft, 1985; Fig. 2A). The areas with lower values of suitability and more resistance to the species displacement were present in southernmost Mexico, the center-north of Venezuela, the Andes, the Sechura Desert in Peru, the Raposa Serra do Sol in Brazil, and northernmost Bolivia (Fig. 2A, B). The broad areas found to be potentially suitable for Blue-crowned Manakins reflect environmental heterogeneity along its known distribution. Most of the highly suitable areas for the species were in places where its occurrence is known.

Least-cost corridors simulated with the species' actual occurrences revealed several current potential corridors among all ecoregions considered in this study (Fig. 2B), except for Branco River, where only a few paths were predicted with low probabilities (Fig. 2C). These corridors presented possible routes of gene flow throughout the Napo area of endemism (sensu Da Silva et al., 2005), linking populations from the trans-Andean region to those from the Amazon basin, particularly along the Marañon-Solimões-Amazonas rivers. However, potential routes of gene flow derived from climatic suitability were somehow disrupted along the Japurá River eastwards the Negro River (within the Jaú area of endemism; sensu Borges & Da Silva, 2012), and highly interrupted to the west, within the Juami-Japurá interfluve (Fig. 2C). The corridors created with random points showed a similar pattern than the ones with the actual data but were broader in the eastern parts of Amazonia (Fig. 2D).

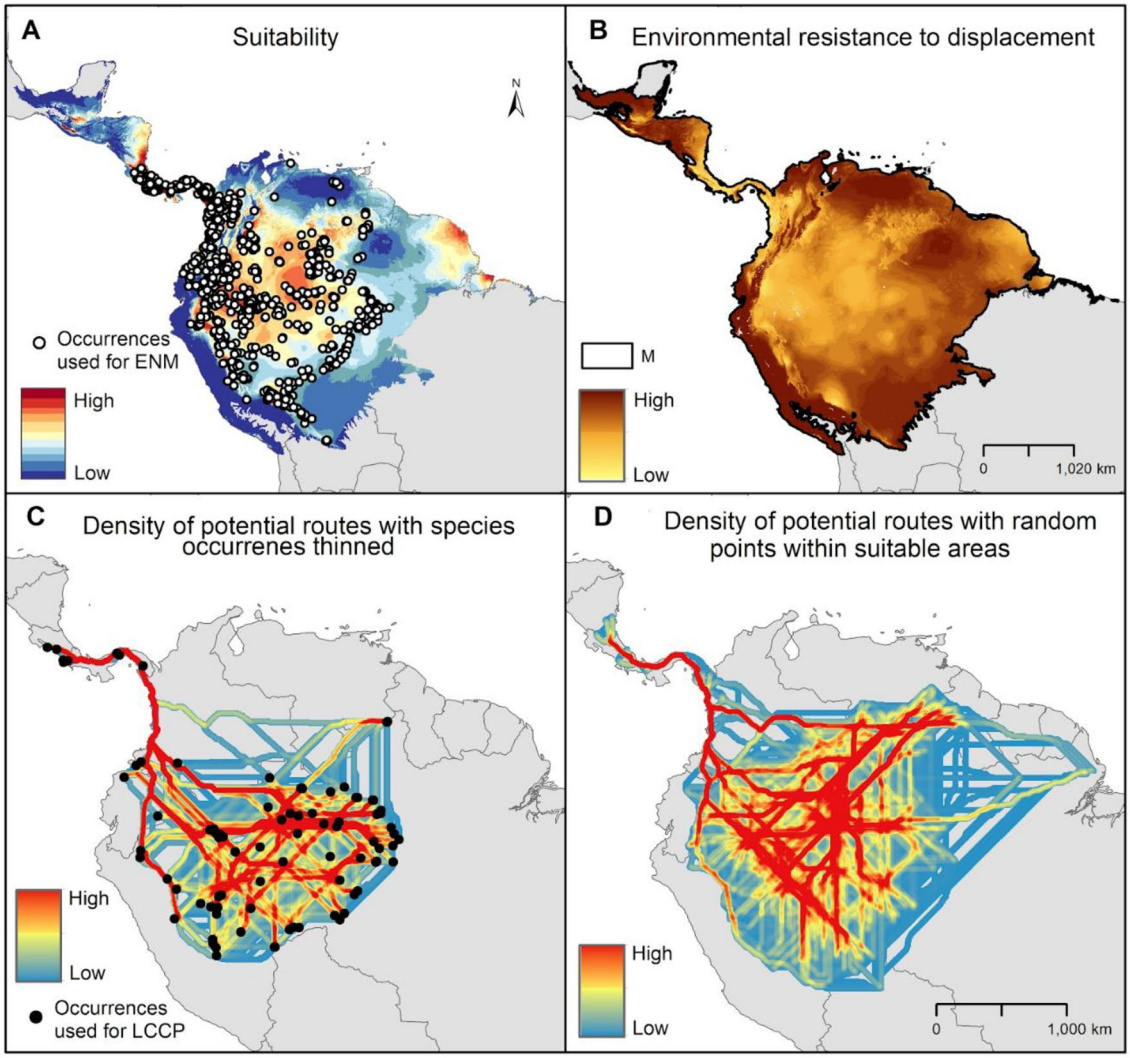

Fig. 2 Results from ecological niche modeling (ENM) and least-cost corridors path analyses (LCCP). **A** Potential suitability for *Lepidothrix coronata*. **B** Friction layer (environmental resistance to displacement; values range from 0 to 10). **C** Potential routes of movements simulated with the actual species' occurrences. **D** Potential routes of movements simulated with 5 sets of 88 random points, each generated inside the potentially suitable areas for this species. The black outline in B represents the calibration area (**M**) (Color figure online)

Phylogenetic Reconstruction and Haplotype Networks

In the two phylogenetic trees (one with the concatenated data set and one species tree; Fig. 3A) we found, with the highest support (PP = 1.0), that *L. coronata* is a monophyletic group, although relationships among lineages recovered within the species were different between those trees, as detailed further below. We recovered four well-supported and geographically structured lineages: (a) Trans-Andean lineage, distributed west of the extreme north of Andes cordillera; (b) Northern Amazonia lineage, present north of the Amazon River, in the Japurá-Negro and Negro-Branco interfluvia, bounded by the Solimões River to the south and the Japurá River to the west, up to the northern parts of the state of Amazonas (Brazil) and Venezuela; (c) Japurá lineage, distributed in Japurá-Solimões interfluve to northern Peru; and (d) Southern Amazonia lineage, delimited by the Solimões-Amazon rivers to the north and extending to the Purus-Madeira interfluvium in the easternmost limit of the distribution of the species.

The concatenated tree showed the Trans-Andean lineage diverging from other lineages about 3.59 million years ago (mya) and Northern Amazonia lineage diverging from the Japurá and Southern Amazonia lineages from about 2.91 mya, both during the Pliocene, whereas the Japurá and Southern Amazonia lineages diverged between each other about 2.39 mya. The onset of the Trans-Andean lineage diversification was ~ 0.77 mya, ~ 1.45 mya for the Northern Amazonia, ~ 1.27 mya for the Japurá, and ~ 1.10 mya for

the Southern Amazonia lineages, during the Pleistocene (Fig. 3A.I). The species tree showed the same topology from the concatenated tree, but did not support monophyly of lineages distributed in the Amazon Basin. According to this tree, the Trans-Andean lineage diverged from the other ~ 2.06 mya and Northern Amazonia from the Southern Amazonia and Japurá lineages ~ 1.88 mya; whereas the Southern Amazonia and Japurá lineages diverged ~ 1.39 mya, all during the Pleistocene (Fig. 3A.II).

The haplotype networks showed a high genetic structure between the trans and cis-Andean lineages, and considerable haplotype sharing among lineages distributed in the Amazonia basin, both for nuclear and mitochondrial molecular markers. There were more individuals sequenced for the mtDNA than nuDNA markers, with similar sequence length among most markers (mean 400 + 136 bp, range 167 bp for ND3 to 612 bp for MYO2). The number of segregation sites was generally higher for mtDNA as well, which presented higher haplotype and nucleotide diversity indices, besides higher number of pairwise differences among individuals in comparison to the nuDNA markers, particularly for G3PDH, whereas MYO2 and FIB5 presented haplotype and nucleotide diversities comparable to those from mtDNA markers (Table S4).

The haplotype network based on the mtDNA revealed similar topology among markers, with four strongly supported lineages with marked phylogeographic structure (Fig. 3B). However, despite the several mutational steps between haplogroups (mainly by COI and CYTB), several median vectors indicate non-sampled or extinct ancestral sequences, highlighted for the CYTB, ND2, and ND3 haplotype networks (Fig. 3B). In general, the trans-Andean lineage agrees with the trans-Andean ecoregions haplogroup (Fig. 3C), emerging with distinct haplotypes compared with other ecoregions identified for all markers except for the COI, which was missing for these samples, which agrees with the splitting between Trans- and Cis-Andean clades in two distinct species (Moncrieff et al., 2022). Almost all haplotypes from the Japurá ecoregion were identified to belong exclusively to the Japurá lineage (Fig. 3C). Nonetheless, the Japurá ecoregion presents haplotypes shared with closely regions, such as southwestern Amazonia (CYTB only), Negro, and Branco (COI, ND2 and ND3). In this sense, Branco and Negro ecoregions presented haplotype sharing for all mtDNA networks except by CYTB, although with few mutational steps between them (Fig. 3C). Considering the Bayesian concatenated tree, the Southern Amazonia lineage was the main widespread clade, corresponding to three distinct ecoregions: Juruá, Purus-Madeira, and Southwest Amazonia (Fig. S2). Overall, the revealed haplogroups were almost supported to the same ecoregion except for networks revealed by CYTB and ND2, which showed haplotype sharing more frequently among these three ecoregions. In addition, few haplotypes were shared across distinct ecoregions (Fig. 3C).

The nuDNA network revealed low-frequency haplotypic variants for FIB5 and G3PDH, with a reticulate evolutionary relationship. However, nuclear haplotype H1 for MYO2 was present in almost all ecoregions and clades revealed by the concatenated phylogenetic time-tree (except Trans-Andean, which was not sampled for this marker). Furthermore, MYO2 haplotype network was the only one that presented a star-like topology among networks. However, mostof haplotypes differed by one substitution site for nuDNA. Except by FIB5 with a weak association of haplotypes and ecoregions, none of phylogenetic lineages was recovered for the nuclear sequences or the same associated directly with a proposed ecoregion (Fig. 3B).

One mtDNA marker (ND2) and two of the nuDNA markers (MYO2 and FIB5) departed from neutrality for Fu's Fs tests, and MYO2 departed also for the Tajima's D test, whereas all other markers did not depart from neutrality. In general, Tajima's D and Fu's Fs tests were negative and non-significant for mtDNA sequences. Negative values from both tests may be interpreted as excess of rare mutations, however the excess is statistically non-significant. Yet, only the ND3 depicted significant P values in Fu' Fs test (-21.79, $P < 0.01$). In contrast, the CYTB marker showed positive values for Tajima's D test (0.47, $P > 0.05$), compatible with a sudden population contraction or balancing selection due to an excess of low-frequency polymorphisms relative to expectation. Furthermore, all nuclear markers (MYO2, FIB5 and G3PDH) showed significant P values for Fu's Fs tests performed on nuDNA, as expected from events of recent population expansion or from genetic hitchhiking, due to evidence for an excess number of alleles. Although presenting negative values, only MYO2 was significant for Tajima's D through nuDNA, due verified excess of rare alleles or recent population expansion (Table S4).

Plumage Patterns

Among the 259 specimens with spectra measurements from plumage regions, variation among the five body plumage patterns was concentrated in the southern portion of the species' range (southern Amazon). A few specimens in almost-black plumages were also found north of the Amazon-Solimões River in southern Ecuador, northern Peru, and in western and northern Brazilian Amazonia (Fig. 1B). Within southern Amazonia, green-bodied males were predominantly found in both the western and eastern extremes of the species distribution, along the left banks of the Ucayali and Madeira rivers, respectively; the other four phenotypes were found patchily distributed across this region. The Ucayali River presented the highest variation in male body plumage patterns, concentrated mainly in its medium and upper

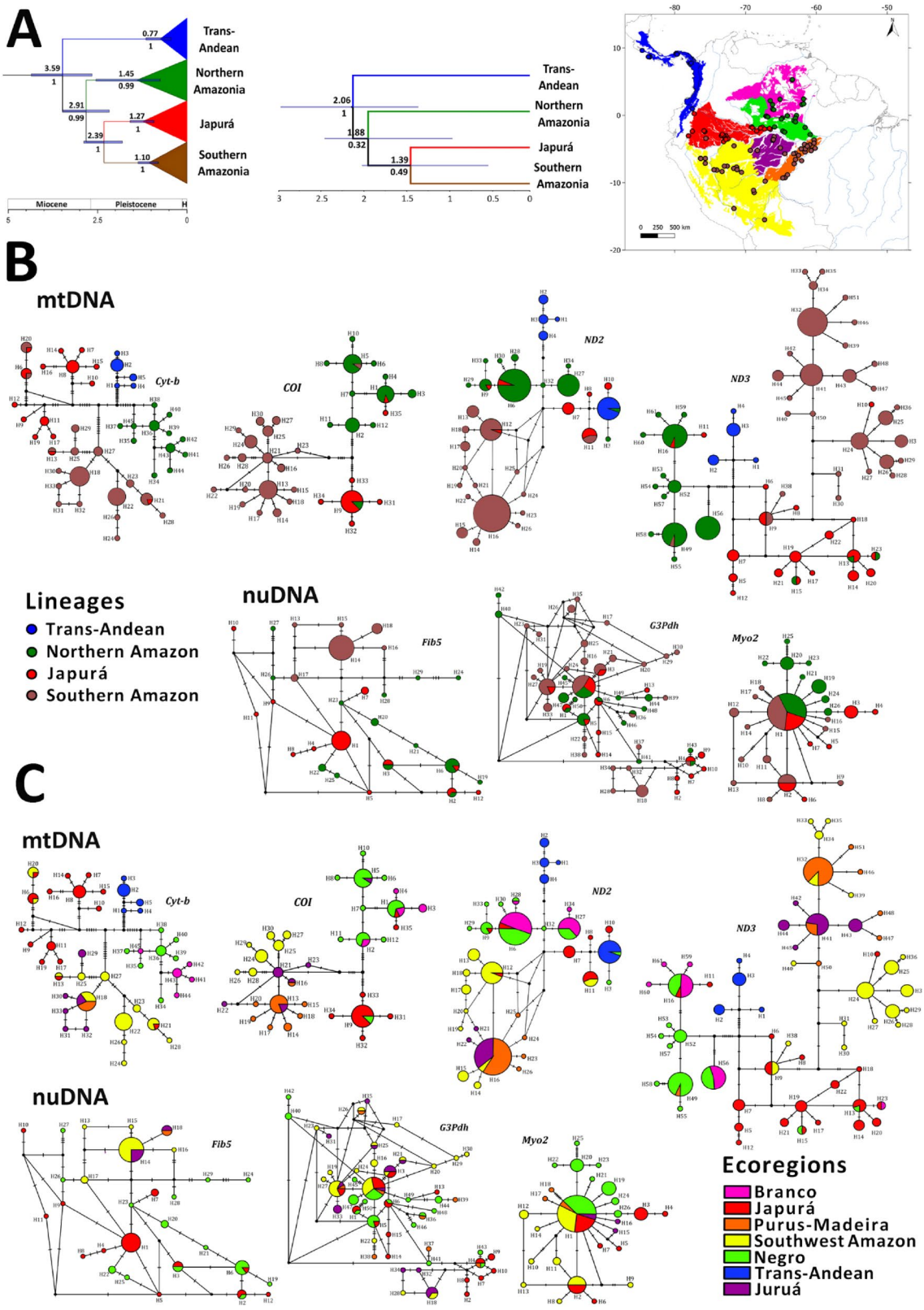

parts, where all five phenotypes were found; it was followed by the Juruá River, with four phenotypes distributed along its banks, but in non-clinal variation. Thus, intermediate plumages were found uniquely in its upper and lower portions; green plumages were found locally in the middle and almost black in the upper portions; whereas black-bodied

◂**Fig. 3** **A** Phylogenetic hypotheses for *Lepidothrix coronata* based on mtDNA and nuDNA for the (I) concatenated dataset and (II) species tree, showing recovered lineages and their distributions (color coded) across Central and South America; **B** Haplotype networks for each molecular marker used in the study (CYTB split in two sets, section "Materials and Methods") showing shared haplotypes among localities from each lineage (points in map colored according to lineages in **A**); **C** Haplotype networks for each molecular marker used in the study (CYTB split in two sets, see section "Materials and Methods") showing shared haplotypes among localities from different ecoregions (colored shapes) adapted from Dinerstein et al. (2017) (Color figure online)

males were found on the left bank along all portions of this river. In turn, the Purus-Madeira interfluvium presented a clinal variation in plumage patterns, particularly in the north, with almost all black plumages found in males from populations close to populations with males in intermediate, almost green and green plumages; whereas only green plumages were found further to the south in this interfluvium, and also in the southern limits of the species distribution (Fig. 2B). Thus, males from all trans-Andean populations were exclusively black. Specimens representing each plumage pattern are shown in Fig. 1C.

Geographic and Environmental Associations with Genetic Variation and Male Plumage Coloration

Most variables were not related to each other in the SEM analysis (Table 2, Fig. 4). Environmental variation was not predicted by latitude ($R^2 = 0.092$, $P = 0.275$), but it was by longitude ($R^2 = 0.315$, $P < 0.001$). Coloration was marginally related to latitude ($R^2 = -0.209$, $P = 0.052$; Table 2, Fig. 4). In the MMRR analysis, no relationship was found between the color and the analyzed predictors (environmental, geographic and least cost distances, for more details see Table 3). Geographic distance, on the other hand, was the best predictor of genetic distance across the species' range ($R^2 = 0.226$, $P < 0.001$), followed by least-cost distance ($R^2 = 0.134$, $P < 0.001$) and the environmental distance ($R^2 = 0.04$, $P < 0.001$) in single variable MMRR models.

Discussion

The phylogenetic reconstruction based on the concatenated data set recovered four well-supported lineages (Japurá, Northern Amazonia, Southern Amazonia, and Trans-Andean), matching the distribution and inter-lineage relationships found for the species in the mtDNA topology of Reis et al. (2020). In turn, the species tree showed the same topology among lineages, though rather weakly supported. This difference was due to the different partition sets for the mtDNA markers that needed to be implemented to run StarBEAST2. Thus, when only the coding markers were used, no relationship among lineages could be supported in the species tree, although the addition of the introns in the analyses resolved the node grouping the Northern Amazonia and Japurá lineages. Our results for the concatenated tree showed the Trans-Andean lineage as sister to all the Amazonia lineages, suggesting that the diversification of the species within the Amazon basin occurred following the uplift of the Northern Andes, thus corroborating recent findings (Cheviron et al., 2005; Moncrieff et al., 2022; Reis et al., 2020). This result is also consistent with those for several organisms, including other passerines [e.g., (D'Horta et al., 2013; Fernandes et al., 2014; Lavinia et al., 2019), invertebrates (Zeh et al., 2003), mammals (Cortés-Ortiz et al., 2003), and plants (Luebert & Weigend, 2014)].

Our results show that geographic distance drives genetic diversification among populations of the Blue-crowned Manakin, indicating a major role of isolation by distance (Wright, 1943) in the distribution of genetic variation in this species. Several studies have reported geographic distance as an important driver of genetic structuring in vertebrates (e.g., Peterson, 1991; Ferreira et al., 2020; Fernandes et al., 2021; review in Sexton et al., 2014). This pattern suggests that physical barriers in the landscape likely play a secondary, or more localized, role in restricting gene flow in the species, decreasing gene flow between populations. Previous studies that showed rivers as drivers of genetic structuring in the Blue-crowned Manakin (Cheviron et al., 2005; Reis et al., 2020) were conducted with coarser sampling scales and framed in biogeographic contexts via phylogeographic approaches. However, when we looked at the population level, geographic distance alone explained the distribution of genetic diversity within the species. To test our hypotheses, we employed both MMRR and SEM analyses. Although an apparent disparity emerged between the two approaches, SEM is the more appropriate model, as it takes into account both direct and indirect relationships simultaneously. While MMRR is typically utilized for less intricate scenarios, we retained this analysis when the causal factors are unequivocal, such as to elucidate the impact of linear geographic distance on genetics and plumage coloration.

Recently, Ramírez-Barrera et al. (2019) identified the effects of long-distance movement and local dispersal (e.g., Malpica & Ornelas, 2014) as main drivers of genetic diversification in the Red-crowned Ant Tanager (*Habia rubica*), and suggested effects of IBD combined with vicariance from tectonic plates and past climatic changes (e.g., Coyne & Orr, 2004; Rull, 2011) in the distribution of genetic diversity in this species. Least-cost corridors based on environmental suitability showed here that the Japurá River was a potential barrier for this species, in agreement with Reis et al. (2020). According to our reconstructions of climatic niches, environmental heterogeneity either connects populations across corridors of suitable habitat or isolates them across regions

Table 2 Results of the structural equation modeling (SEM) analysis, with regressions (PC1 of variable 1 × PC1 of variable 2), testing for predictive power of geographic and environmental variation on phenotypic and genetic variation, and between these two

Model	R^2	P
Env ~ Lat	0.092	0.275
Env ~ Lon	**0.315**	**0.00001**
Col ~ Lat	**− 0.209**	**0.052**
Col ~ Lon	0.028	0.810
Col ~ Env	− 0.004	0.969
Col ~ Gen	− 0.091	0.293
Gen ~ Lat	− 0.167	0.119
Gen ~ Lon	0.162	0.156
Gen ~ Env	− 0.103	0.345

Statistically significant relationships ($P \leq 0.05$) are highlighted in bold

Lat latitude, *Lon* longitude, *Col* coloration, *Gen* genetic, *Env* environment

of interrupted habitat suitability, possibly regulating genetic divergence among lineages. The environmental connectivity found by us in the Napo region considering the current climatic conditions can explain, for example, the complex evolutionary history of the White-crowned Manakin (*Pseudopipra pipra*) reported by Berv et al. (2020) in that area, where populations have undergone hybridization and formed a local lineage through introgression. A recent consensus is that both current and past environmental heterogeneity shaped the diversification and distribution of organisms in the Amazon Basin (Godinho & Da Silva, 2018; Machado et al., 2019; Naka & Brumfield, 2018; Ortiz et al., 2018; Silva et al., 2019). These patterns indicate that a combination of processes is at play in the underlying genetic structuring between lineages across the margins of the major Amazonian rivers. In this context, we found that gene flow among populations of the Blue-crowned Manakin is mostly influenced by the geographic distances between populations.

Plumage coloration, on the other hand, was marginally explained by latitude, thus confirming the overall pattern described for the species of a north-to-south variation in male plumage color. Spectral data show that such is the case for both body and crown plumage in males, although we may not indicate a mechanism driving this variation within those directly tested here. A super black plumage (McCoy & Prum, 2019) has been reported for the two trans-Andean subspecies with black-bodied plumages (*L. c. velutina* and *L. c. minuscula*), which form a clade and have been recently proposed for recognition as a different species from the cis-Andean populations (Moncrieff et al., 2022). In the latter species, populations with black body plumages are paraphyletic, given the records of black-plumaged males in

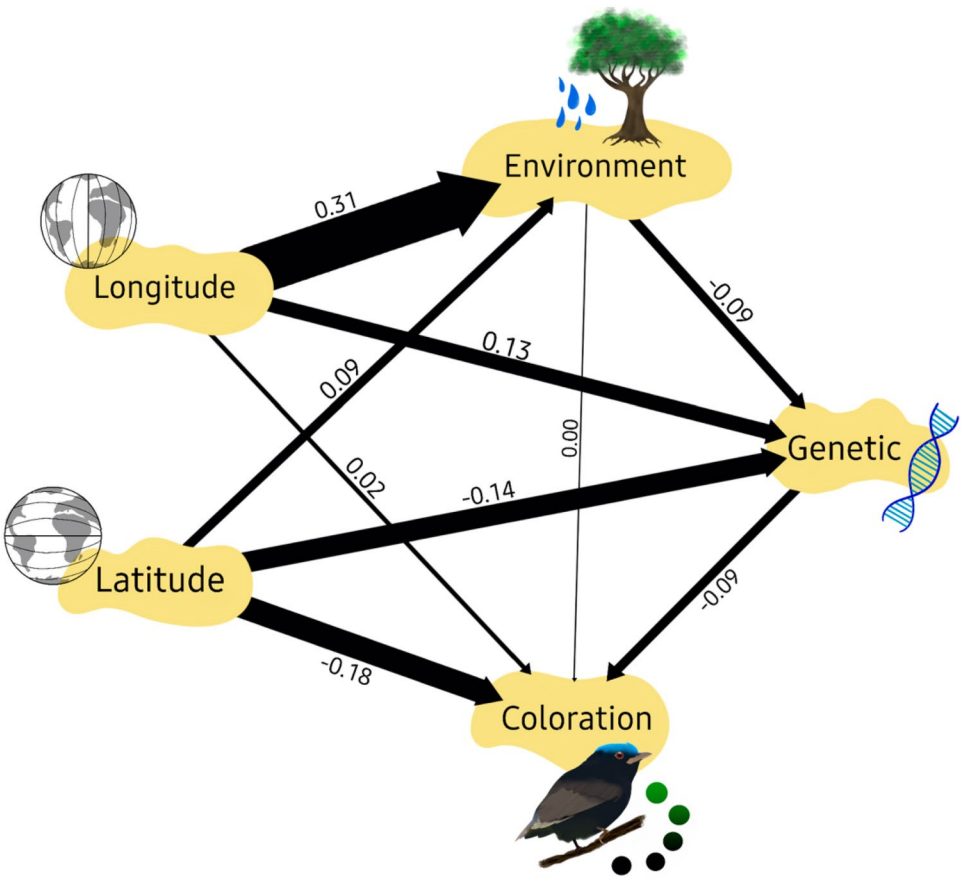

Fig. 4 Results from structural equation modeling showing regression coefficients (proportional to line thickness) among explanatory variables (genetic and coloration) and each predictor variable (environment, latitude and longitude); test significances are shown in Table 2 (Color figure online)

Table 3 Results of multiple matrix regression with randomization (MMRR) (Response variable ~ Predictor variable) relating the linear geographic distance and the least-cost distance to the genetic and coloration distance matrices obtained for *Lepidothrix coronata* from locations sampled

Model		R^2	P
Coloration ~ Predictor	Geography	0.005	0.105
	Least-cost	0.003	0.150
	Environmental	0.003	0.338
Genetic ~ Predictor	**Geography**	**0.226**	**< 0.001**
	Least-cost	**0.134**	**< 0.001**
	Environmental	**0.04**	**< 0.001**

Statistically significant regressions are presented in bold

populations located both west and east of the Purus River (Reis et al., 2020; Fig. 1B). Spectral data showed higher variation in plumage colors than the plumage patterns perceived by the human eye, as spectra provide multidimensional information associated with color data (Stoddard & Prum, 2008), summarized in different metrics that varied within a given plumage pattern. This variation included differences in black plumages between cis- and trans-Andean taxa, and variation in the blue crown coloration, which aligned with taxonomic descriptions (deep purplish blue in males from trans-Andean populations; dark blue in northern Amazon Basin; lighter blue hues in the southern parts of the range, Kirwan & Green, 2011; Appendix S4, Fig. S3A).

In addition to the Amazon River, which limits the distribution of black- and intermediate-plumaged populations in the Central Amazon near Manaus, the Ucayali, and middle Juruá rivers also separate populations of black- and green-plumaged males. In the middle Juruá region, populations with black or almost black plumages occur in the left bank, whereas green-plumaged males occur on the right bank of the river (Mutchler et al., 2020). In the upper Juruá region males with almost black plumages occur on both sides of the river and in the lower Juruá, males with intermediate plumages are also found on both margins. Therefore, the Ucayali and mid-Juruá regions represent examples of local river effects on the diversification of male plumage coloration. In turn, clinal variation within the Purus-Madeira interfluve (Teófilo et al., 2018) and along the Ucayali River (Moncrieff et al., 2022) is suggestive of local selective pressures (e.g. Hoekstra et al., 2004) driving evolution of male plumage coloration. Although a similar clinal geographic pattern can be observed across the entire species' range, adaptive processes inferred elsewhere for the species apply to localized and peculiar spatial configurations of environmental conditions (e.g. Schietti et al., 2016). These findings agree with the geographic variation in male plumage color documented for the species previously (reviews in Anciães et al., 2009; Kirwan & Green, 2011; clinal variation in Teófilo et al., 2018; Moncrieff et al., 2022), and further expands it by providing a map with plumage patterns by population sampled, showing higher degree of geographic variation than previously recognized for the species, with clinal variations locally restricted.

Overall, color patterns suggest phenotypic diversification of body plumages in the south, where the ancestral (black) state is also found. This effect could be mediated by multiple colonization events of black-bodied populations in contact zones with populations from the Japurá and northern regions. Wang and Shaffer (2008) described a similar process for the Strawberry Poison-dart Frog (*Oophaga pumilio*), which presents an unusual pattern of polychromatism. They observed variation in color patterns according to the location: Mainland populations have red coloration, whereas insular populations exhibit an explosion of color morphs, which authors attributed to the formation of islands, given their congruence in time (Anderson & Handley, 2002). Thus, they pointed to multiple colonization events in the archipelago, with the rapid evolution of novel phenotypes associated with strong diversifying selection as a result of different factors (Reynolds & Fitzpatrick, 2007; Siddiqi et al., 2004; Summers et al., 1999).

The lack of association between genetic and color variation observed here and elsewhere (Cheviron et al., 2005, 2006; Reis et al., 2020) indicates that adaptive mechanisms possibly acting on local populations are not isolating populations, as predicted by isolation by adaptation to different environments (IBA, a particular case of IBE; Rundle & Nosil, 2005). IBA is defined as the effect of environmental gradients that cause divergent natural selection, resulting in a positive correlation between genetic divergence and adaptive phenotypic differentiation (Andersson, 1994; Basolo & Endler, 1995; Boughman, 2001; Boul et al., 2007; Hoekstra et al., 2004; Leal & Fleishman, 2004). This correlation occurs when gene flow between populations is restricted by individual partner preferences or by mortality of immigrant phenotypes (Ramírez-Barrera et al., 2019; Rundle & Nosil, 2005). As such, variation in male plumage possibly underlaid genetic diversification, via sexual and/or natural selection as predicted through isolation by adaptation. As Cheviron et al. (2006) suggested, because plumage patterns are under polygenic regulation (Roulin & Ducrest, 2013; review in Kulikova, 2021) and multiple phenotypes are found along contact zones, observed variation might be linked to both genetic and ontogenetic mechanisms, as well as to variation in selective pressures among populations, given their role in sexual selection (Darwin, 1896; Prum, 2012; Servedio & Boughman, 2017).

These findings are partially supported by studies across various taxa, suggesting that geographic isolation plays a primary role in driving both phenotypic and genetic diversification among populations (Fernandes et al., 2014, 2021;

Ferreira et al., 2018, 2020; Kaefer et al., 2013; Naka et al., 2012; Pirani et al., 2019; Ribas et al., 2012; Simões et al., 2014). Additionally, it appears that secondary or overlooked environmental factors also influence these processes. Even though polychromatism is relatively common among birds and anurans, studies pointing to mechanisms driving its distribution are rare (but see above). Rojas et al. (2020) showed that the genetic diversity of the highly polychromatic poison frog *Adelphobates galactonotus* could be explained by geographic isolation from river barriers and climatic oscillations during the Pleistocene. However, neither those factors, nor genetic variation explained observed variation in dorsal coloration among populations, which could reflect local processes. The structural equation modeling implemented here depicted latitudinal effects in plumage color, thus corroborating Fernandes et al. (2021) when suggesting that latitude per se is highly relevant as an ecological and evolutionary driver of the spatial distribution of intraspecific phenotypic diversity.

This study represents one of the pioneering efforts to unravel the drivers behind genetic diversity and variation in male plumage coloration within the Blue-crowned Manakin at a broad geographic scale, within an evolutionary framework. We aimed to investigate the influence of geographic and environmental factors on genetic and morphological diversity. While previous studies have demonstrated associations between these factors and variation in male plumage coloration among populations in specific interfluvial regions, our results reveal that some of these patterns are not consistently observed across the species' entire range, particularly in relation to environmental heterogeneity. However, we found a strong association between genetic diversity among populations and both linear and least-cost geographic distances, highlighting the role of isolation by distance, whether measured in linear or least-cost terms within the environment. Interestingly, we did not find direct evidence of environmental heterogeneity playing a significant role in genetic isolation. Our findings also suggest the absence of clear evidence for adaptive evolution, aligning with previous phylogenetic studies that reported a lack of correlation between genetic diversity and color variation. We propose that genetic drift plays a crucial role in driving genetic differentiation at the regional scale, while both stochastic and deterministic factors operate at local scales in shaping the evolution of male Blue-crowned Manakins' plumage coloration.

Supplementary Information The online version contains supplementary material available at https://doi.org/10.1007/s11692-023-09613-4.

Acknowledgements We thank the curators from the following institutions for providing samples: INPA, MPEG, MZUSP, MHNNKM, LSUMNS, AMNH, and USNM. Jaqueline Fortuna and Camila Reis shared sequences produced during their studies supervised by MA and PSR respectively. We are grateful to Romina Batista, Fernanda Werneck, Ana Carolina Carnaval, Pedro Ivo Simões, Alexandre Mendes Fernandes, Fabrício Skupien, Pedro Sena, and Renato Salomão for helpful comments on the manuscript. We thank Ivan Prates, André Lira, and Victor Leandro-Silva for statistical support. We thank Laura Schaedler and Fabricio Furni for their English review and the editors and anonymous reviewers for their valuable contributions to the manuscript. Conselho Nacional de Desenvolvimento Científico e Tecnológico (CNPq) provided masters fellowship to PP (132256/2018-5); productivity grants to ILK, JA (439040/2018-3) and PSR (311539/2019-0); DCR fellowship and Universal research Grant (MCTI/CNPq 471092/2006-06) to MA. Fundação de Amparo à Pesquisa do Estado do Amazonas provided DCR (DCR/FAPEAM/CNPq 020/2006), PPP (PPP/FAPEAM/CNPq 012/2008) and PRONEX Grants (PRONEX/FAPEAM/CNPq 003/2009) to MA; and SISBIOTA network research fund (SISBIOTA/FAPEAM/CNPq 563348/2010-0) to IPF. Coordenação de Aperfeiçoamento de Pessoal de Nıível Superior—Brasil (CAPES) granted PSR (88881.337398/2019-01). The National Science Foundation provided travel support to PP, CB, AEM, LWL, and MA under Grant No. 1457541, the Manakin Genomics Research Coordination Network. This paper is developed in the context of National Institutes for Science and Technology (INCT) in Ecology, Evolution, and Biodiversity Conservation, supported by MCTIC/CNPq (proc. 465610/2014-5) and FAPEG (proc. 201810267000023).

Author Contributions PP, ILK, and MA conceived and designed the project. ATP, IPF and TH provided conceptual and logistic support. PSR, CD and AA contributed with genetic data, analyses and discussing results. PP organized the study, compiled all data, ran environmental (SDM), color and statistical (MMRR) analyses, led writing and author contributions. LWL and MB ran PCA (genetic and color) inputs for statistical (SEM) analyses carried out by IYF. MA, SH and CD conducted labwork and generated the genetic data. CB, EP. WTP and AFM carried the genetic analyses. FHT and AEM collected spectral data, assisted in color analysis and interpretation of results. LNB, and AFM helped in environmental analyses, CN-P generated LCCPs and APR produced the maps. All authors revised the manuscript at least once and made contributions to the present version.

Data Availability The authors declare that the data supporting the findings of this study are available within the article and its supplementary information files. Raw data were generated at the Genetic and Evolution Lab from the Federal University of Amazonas (UFAM) by the anchor author and several co-authors. With that, derived data supporting the findings of this study are available from the corresponding author upon request. Sequence data will be deposited in a repository free of change upon manuscript publication, to protect authors' rights and concerns.

Declarations

Conflict of interest The authors declare no conflict of interest.

References

Aiello-Lammens, M. E., Boria, R. A., Radosavljevic, A., Vilela, B., & Anderson, R. P. (2015). spThin: An R package for spatial thinning of species occurrence records for use in ecological niche models. *Ecography*, *38*(5), 541–545.

Amézquita, A., Lima, A. P., Jehle, R., Castellanos, L., Ramos, Ó., Crawford, A. J., Gasser, H., & Hödl, W. (2009). Calls, colours, shape, and genes: A multi-trait approach to the study of

geographic variation in the Amazonian frog *Allobates femoralis*. *Biological Journal of the Linnean Society, 98*(4), 826–838. https://doi.org/10.1111/j.1095-8312.2009.01324.x

Anciães, M., Durães, R. R., Cerqueira, M. C., Fortuna, J. R., Sohn, N., Cohn-haft, M., & Farias, I. P. (2009). Diversidade de Piprideos (Aves: Pipridae) Amazônicos: Seleção sexual, ecologia e evolução. *Oecologia Brasiliensis, 13*(1), 165–182.

Anderson, R. P., & Handley, C. O. (2002). Dwarfism in insular sloths: Biogeography, selection, and evolutionary rate. *Evolution, 56*(5), 1045–1058. https://doi.org/10.1111/j.0014-3820.2002.tb01415.x

Anderson, R. P., Lew, D., & Peterson, A. T. (2003). Evaluating predictive models of species' distributions: Criteria for selecting optimal models. *Ecological Modelling, 162*(3), 211–232. https://doi.org/10.1016/S0304-3800(02)00349-6

Andersson, M. (1994). *Sexual selection*. Princeton University Press.

Barve, N., Barve, V., Jiménez-Valverde, A., Lira-Noriega, A., Maher, S. P., Peterson, A. T., Soberón, J., & Villalobos, F. (2011). The crucial role of the accessible area in ecological niche modeling and species distribution modeling. *Ecological Modelling, 222*(11), 1810–1819. https://doi.org/10.1016/j.ecolmodel.2011.02.011

Basolo, A. L., & Endler, J. A. (1995). Sensory biases and the evolution of sensory systems. *Trends in Ecology & Evolution, 10*(12), 489.

Becker, R. A., Wilks, A. R., Brownrigg, R., Minka, T. P., & Deckmyn, A. (2021). Maps: Draw geographical maps. *R package version,* 3.4.0. https://CRAN.R-project.org/package=maps

Benites, P., Eaton, M. D., García-Trejo, E. A., & Navarro-Sigüenza, A. G. (2020). Environment influences the geographic phenotypic variation in Velazquez's Woodpecker (*Centurus santacruzi*). *Journal of Ornithology, 161*(3), 621–634. https://doi.org/10.1007/s10336-020-01748-x

Berv, J. S., Campagna, L., Feo, T. J., Castro-Astor, I., Ribas, C. C., Prum, R. O., & Lovette, I. J. (2020). Genomic phylogeography of the white crowned manakin *Pseudopipra pipra* (Aves: Pipridae) illuminates a continental-scale radiation out of the Andes. *bioRxiv*. https://doi.org/10.1101/713081

Bivand, R., Keitt, T., Rowlingson, B., Pebesma, E., Sumner, M., Hijmans, R., Rouault, E., & Bivand, M. R. (2015). Package 'rgdal'. *Bindings for the Geospatial Data Abstraction Library*. https://cran.r-project.org/web/packages/rgdal/index.html

Bivand, R., Rundel, C., Pebesma, E., Stuetz, R., Hufthammer, K. O., & Bivand, M. R. (2017). Package 'rgeos'. *The Comprehensive R Archive Network (CRAN)*.

Borges, S. H., & Da Silva, J. M. C. (2012). A new area of endemism for Amazonian birds in the Rio Negro Basin. *Wilson Journal of Ornithology, 124*(1), 15–23. https://doi.org/10.1676/07-103.1

Bouckaert, R., Heled, J., Kühnert, D., Vaughan, T., Wu, C. H., Xie, D., Suchard, M. A., Rambaut, A., & Drummond, A. J. (2014). BEAST 2: A software platform for Bayesian evolutionary analysis. *PLoS Computational Biology, 10*(4), e1003537. https://doi.org/10.1371/journal.pcbi.1003537

Boughman, J. W. (2001). Divergent sexual selection enhances reproductive isolation in sticklebacks. *Nature, 411*(6840), 944–948. https://doi.org/10.1038/35082064

Boul, K. E., Funk, W. C., Darst, C. R., Cannatella, D. C., & Ryan, M. J. (2007). Sexual selection drives speciation in an Amazonian frog. *Proceedings of the Royal Society B: Biological Sciencess, 274*(1608), 399–406. https://doi.org/10.1098/rspb.2006.3736

Brown, J. L., Bennett, J. R., & French, C. M. (2017). SDMtoolbox 2.0: The next generation Python-based GIS toolkit for landscape genetic, biogeographic and species distribution model analyses. *PeerJ, 5*, e4095. https://doi.org/10.7717/peerj.4095

Cadena, C. D., Cheviron, Z. A., & Funk, W. C. (2011). Testing the molecular and evolutionary causes of a "leapfrog" pattern of geographical variation in coloration. *Journal of Evolutionary Biology, 24*(2), 402–414. https://doi.org/10.1111/j.1420-9101.2010.02175.x

Chan, L. M., Brown, J. L., & Yoder, A. D. (2011). Integrating statistical genetic and geospatial methods brings new power to phylogeography. *Molecular Phylogenetics and Evolution, 59*(2), 523–537. https://doi.org/10.1016/j.ympev.2011.01.020

Chesser, R. T. (1999). Molecular systematics of the rhinocryptid genus *Pteroptochos*. *Condor, 101*(2), 439–446. https://doi.org/10.2307/1370012

Cheviron, Z. A., Hackett, S. J., & Brumfield, R. T. (2006). Sequence variation in the coding region of the melanocortin-1 receptor gene (MC1R) is not associated with plumage variation in the blue-crowned manakin (*Lepidothrix coronata*). *Proceedings of the Royal Society B: Biological Sciences, 273*(1594), 1613–1618. https://doi.org/10.1098/rspb.2006.3499

Cheviron, Z. A., Hackett, S. J., & Capparella, A. P. (2005). Complex evolutionary history of a Neotropical lowland forest bird (*Lepidothrix coronata*) and its implications for historical hypotheses of the origin of Neotropical avian diversity. *Molecular Phylogenetics and Evolution, 36*(2), 338–357. https://doi.org/10.1016/j.ympev.2005.01.015

Cobos, M. E., Jiménez, L., Nuñez-Penichet, C., Romero-Alvarez, D., & Simões, M. (2018). Sample data and training modules for cleaning biodiversity information. *Biodiversity Informatics, 13*, 49–50. https://doi.org/10.17161/bi.v13i0.7600

Cobos, M. E., Peterson, A. T., Barve, N., & Osorio-Olvera, L. (2019). kuenm: An R package for detailed development of ecological niche models using Maxent. *PeerJ, 7*, e6281. https://doi.org/10.7717/peerj.6281

Corander, J., Marttinen, P., Sirén, J., & Tang, J. (2013). *BAPS: Bayesian analysis of population structure* (p. 14). Department of Mathematics and Statistics University of Helsinki.

Cortés-Ortiz, L., Bermingham, E., Rico, C., Rodrıguez-Luna, E., Sampaio, I., & Ruiz-Garcıa, M. (2003). Molecular systematics and biogeography of the Neotropical monkey genus, *Alouatta*. *Molecular Phylogenetics and Evolution, 26*(1), 64–81. https://doi.org/10.1016/S1055-7903(02)00308-1

Coyne, J. A., & Orr, H. A. (2004). *Speciation* (Vol. 37). Sinauer Associates.

Cracraft, J. (1985). Historical biogeography and patterns of differentiation within the South American avifauna: Areas of endemism. *Ornithological Monographs*, 49–84.

D'Horta, F. M., Cuervo, A. M., Ribas, C. C., Brumfield, R. T., & Miyaki, C. Y. (2013). Phylogeny and comparative phylogeography of *Sclerurus* (Aves: Furnariidae) reveal constant and cryptic diversification in an old radiation of rain forest understorey specialists. *Journal of Biogeography, 40*(1), 37–49. https://doi.org/10.1111/j.1365-2699.2012.02760.x

Da Silva, J. M. C., Rylands, A. B., & Da Fonseca, G. A. (2005). O destino das áreas de endemismo da Amazônia. *Megadiversidade, 1*(1), 124–131.

Darwin, C. (1896). *Charles Darwin's works: The descent of man and selection in relation to sex* (Vol. 9). D. Appleton.

Del Hoyo, J., Elliott, A., Sargatal, J., Collar, N. J., & Cabot, J. (2004). *Handbook of the birds of the world: Cotingas to pipits and wagtails* (Vol. 9). Lynx Edicions.

Dias, C., de Araújo Lima, K., Araripe, J., Aleixo, A., Vallinoto, M., Sampaio, I., Schneider, H., & do Rêgo, P. S. (2018). Mitochondrial introgression obscures phylogenetic relationships among manakins of the genus *Lepidothrix* (Aves: Pipridae). *Molecular Phylogenetics and Evolution, 126*, 314–320. https://doi.org/10.1016/j.ympev.2018.04.017

Dinerstein, E., Olson, D., Joshi, A., Vynne, C., Burgess, N. D., Wikramanayake, E., Hahn, N., Palminteri, S., Hedao, P., Noss, R., & Hansen, M. (2017). An ecoregion-based approach to

protecting half the terrestrial realm. *BioScience, 67*(6), 534–545. https://doi.org/10.1093/biosci/bix014

Doyle, J., & Doyle, J. (1987). *A rapid DNA isolation procedure for small quantities of fresh leaf tissue* (No. Research).

Eaton, M. D. (2005). Human vision fails to distinguish widespread sexual dichromatism among sexually "monochromatic" birds. *Proceedings of the National Academy of Sciences of the United States of America, 102*(31), 10942–10946. https://doi.org/10.1073/pnas.0501891102

Edgar, R. C. (2004). MUSCLE: Multiple sequence alignment with high accuracy and high throughput. *Nucleic Acids Research, 32*(5), 1792–1797. https://doi.org/10.1093/nar/gkh340

Escobar, L. E., Lira-Noriega, A., Medina-Vogel, G., & Peterson, A. T. (2014). Potential for spread of the white-nose fungus (*Pseudogymnoascus destructans*) in the Americas: Use of Maxent and NicheA to assure strict model transference. *Geospatial Health*. https://doi.org/10.4081/gh.2014.19

Excoffier, L., & Lischer, H. E. L. (2010). Arlequin suite ver 3.5: A new series of programs to perform population genetics analyses under Linux and Windows. *Molecular Ecology Resources, 10*(3), 564–567. https://doi.org/10.1111/j.1755-0998.2010.02847.x

Fernandes, A. M., Wink, M., Sardelli, C. H., & Aleixo, A. (2014). Multiple speciation across the Andes and throughout Amazonia: The case of the spot-backed antbird species complex (*Hylophylax naevius/Hylophylax naevioides*). *Journal of Biogeography, 41*(6), 1094–1104. https://doi.org/10.1111/jbi.12277

Fernandes, I. Y., Moraes, L. J., Menin, M., Farias, I. P., Lima, A. P., & Kaefer, I. L. (2021). Unlinking the speciation steps: Geographical factors drive changes in sexual signals of an Amazonian nurse-frog through body size variation. *Evolutionary Biology, 48*(1), 81–93.

Ferreira, A. S., Jehle, R., Stow, A. J., & Lima, A. P. (2018). Soil and forest structure predicts large-scale patterns of occurrence and local abundance of a widespread Amazonian frog. *PeerJ, 2018*(8), 1–26. https://doi.org/10.7717/peerj.5424

Ferreira, A. S., Lima, A. P., Jehle, R., Ferrão, M., & Stow, A. (2020). The influence of environmental variation on the genetic structure of a poison frog distributed across continuous Amazonian rainforest. *Journal of Heredity, 111*(5), 457–470. https://doi.org/10.1093/jhered/esaa034

Fu, Y. X. (1997). Statistical tests of neutrality of mutations against population growth, hitchhiking and background selection. *Genetics, 147*(2), 915–925.

Furrer, R., Nychka, D., Sain, S., & Nychka, M. D. (2009). *Package 'fields.'* R Foundation for Statistical Computing.

Godinho, M. B. C., & Da Silva, F. R. (2018). The influence of riverine barriers, climate, and topography on the biogeographic regionalization of Amazonian anurans. *Scientific Reports, 8*(1), 1–11. https://doi.org/10.1038/s41598-018-21879-9

Goldsmith, T. H. (1990). Optimization, constraint, and history in the evolution of eyes. *Quarterly Review of Biology, 65*(3), 281–322. https://doi.org/10.1086/416840

Hackett, S. J. (1996). Molecular phylogenetics and biogeography of tanagers in the genus *Ramphocelus* (Aves). *Molecular Phylogenetics and Evolution, 5*(2), 368–382. https://doi.org/10.1006/mpev.1996.0032

Hellmayr, C. E. (1907). On a collection of birds from Teffé, Rio Solimões, Brazil. *Novitates Zoologicae, 14*(1), 40–91.

Hijmans, R. J., Cameron, S. E., Parra, J. L., Jones, P. G., & Jarvis, A. (2005). Very high resolution interpolated climate surfaces for global land areas. *International Journal of Climatology, 25*(15), 1965–1978. https://doi.org/10.1002/joc.1276

Hijmans, R. J., Van Etten, J., Cheng, J., Mattiuzzi, M., Sumner, M., Greenberg, J. A., Lamigueiro, O. P., Bevan, A., Racine, E. B., Shortridge, A., & Hijmans, M. R. J. (2015). Package 'raster'. *R package*, *734*.

Hoekstra, H. E., Drumm, K. E., & Nachman, M. W. (2004). Ecological genetics of adaptive color polymorphism in pocket mice: Geographic variation in selected and neutral genes. *Evolution, 58*(6), 1329–1341. https://doi.org/10.1111/j.0014-3820.2004.tb01711.x

Huson, D. H., & Bryant, D. (2006). Application of phylogenetic networks in evolutionary studies. *Molecular Biology and Evolution, 23*(2), 254–267. https://doi.org/10.1093/molbev/msj030

Ivanova, N. V., Zemlak, T. S., Hanner, R. H., & Hebert, P. D. (2007). Universal primer cocktails for fish DNA barcoding. *Molecular Ecology Notes, 7*(4), 544–548. https://doi.org/10.1111/j.1471-8286.2007.01748.x

Jolliffe, I. T. (1986). Principal components in regression analysis. In *Principal component analysis* (pp. 129–155). Springer. https://doi.org/10.1007/978-1-4757-1904-8_8

Kaefer, I. L., Tsuji-Nishikido, B. M., Mota, E. P., Farias, I. P., & Lima, A. P. (2013). The early stages of speciation in Amazonian forest frogs: Phenotypic conservatism despite strong genetic structure. *Evolutionary Biology, 40*(2), 228–245. https://doi.org/10.1007/s11692-012-9205-4

Kirwan, G. M., & Green, G. (2011). *Cotingas and manakins*. Princeton University Press.

Kulikova, I. V. (2021). Molecular mechanisms and gene regulation of melanic plumage coloration in birds. *Russian Journal of Genetics, 57*(8), 893–911.

Lanfear, R., Calcott, B., Ho, S. Y., & Guindon, S. (2012). PartitionFinder: Combined selection of partitioning schemes and substitution models for phylogenetic analyses. *Molecular Biology and Evolution, 29*(6), 1695–1701. https://doi.org/10.1093/molbev/mss020

Lanfear, R., Frandsen, P. B., Wright, A. M., Senfeld, T., & Calcott, B. (2017). PartitionFinder 2: New methods for selecting partitioned models of evolution for molecular and morphological phylogenetic analyses. *Molecular Biology and Evolution, 34*(3), 772–773. https://doi.org/10.1093/molbev/msw260

Lavinia, P. D., Barreira, A. S., Campagna, L., Tubaro, P. L., & Lijtmaer, D. A. (2019). Contrasting evolutionary histories in Neotropical birds: Divergence across an environmental barrier in South America. *Molecular Ecology, 28*(7), 1730–1747. https://doi.org/10.1111/mec.15018

Leal, M., & Fleishman, L. J. (2004). Differences in visual signal design and detectability between dllopatric populations of *Anolis* lizards. *American Naturalist, 163*(1), 26–39. https://doi.org/10.1086/379794

Lee, K. H., Shaner, P. J. L., Lin, Y. P., & Lin, S. M. (2016). Geographic variation in advertisement calls of a microhylid frog—Testing the role of drift and ecology. *Ecology and Evolution, 6*(10), 3289–3298. https://doi.org/10.1002/ece3.2116

Leite, R. N., Kimball, R. T., Braun, E. J., Derryberry, E. P., Hosner, P. A., Derryberry, G. E., Anciães, M., McKay, J. S., Aleixo, A., Ribas, C. C., Brumfield, R. T., & Cracraft, J. (2020). Phylogenomics of manakins (Aves: Pipridae) using alternative locus filtering strategies based on informativeness. *Molecular Phylogenetics and Evolution, 155*, 107013. https://doi.org/10.1016/j.ympev.2020.107013

Lewin-Koh, N. J., Bivand, R., Pebesma, J., Archer, E., Baddeley, A., Giraudoux, D. G., Rubio, V. G., Hausmann, P., Hufthammer, K. O., Jagger, T., & Sebastian, P. (2012). Package 'maptools'. http://cran.r-project.org/web/packages/maptools/maptools.pdf

Librado, P., & Rozas, J. (2009). DnaSP v5: A software for comprehensive analysis of DNA polymorphism data. *Bioinformatics, 25*(11), 1451–1452. https://doi.org/10.1093/bioinformatics/btp187

Luebert, F., & Weigend, M. (2014). Phylogenetic insights into Andean plant diversification. *Frontiers in Ecology and Evolution, 2*, 27. https://doi.org/10.3389/fevo.2014.00027

Machado, A. F., Nunes, M. S., Silva, C. R., dos Santos, M. A., Farias, I. P., da Silva, M. N. F., & Anciães, M. (2019). Integrating phylogeography and ecological niche modelling to test diversification hypotheses using a Neotropical rodent. *Evolutionary Ecology, 33*(1), 111–148. https://doi.org/10.1007/s10682-019-09968-1

Maia, G. F., Lima, A. P., & Kaefer, I. L. (2017). Not just the river: Genes, shapes, and sounds reveal population-structured diversification in the Amazonian frog *Allobates tapajos* (Dendrobatoidea). *Biological Journal of the Linnean Society, 121*(1), 95–108. https://doi.org/10.1093/biolinnean/blw017

Maia, R., Gruson, H., Endler, J. A., & White, T. E. (2019). pavo 2: New tools for the spectral and spatial analysis of colour in r. *Methods in Ecology and Evolution, 10*(7), 1097–1107. https://doi.org/10.1111/2041-210X.13174

Malpica, A., & Ornelas, J. F. (2014). Postglacial northward expansion and genetic differentiation between migratory and sedentary populations of the broad-tailed hummingbird (*Selasphorus platycercus*). *Molecular Ecology, 23*(2), 435–452. https://doi.org/10.1111/mec.12614

Mccoy, D. E., & Prum, R. O. (2019). Convergent evolution of super black plumage near bright color in 15 bird families. *Journal of Experimental Biology*. https://doi.org/10.1242/jeb.208140

Moncrieff, A. E., Faircloth, B. C., & Brumfield, R. T. (2022). Systematics of *Lepidothrix* manakins (Aves: Passeriformes: Pipridae) using RADcap markers. *Molecular Phylogenetics and Evolution*. https://doi.org/10.1016/j.ympev.2022.107525

Mutchler, M. J., Costa, B., Hiller, A. E., Lima, G. R., Matinata, B., Salter, J. F., Rego, M., Schimitt, D. C., & Del-Rio, G. (2020). Birds of the Juruá River—Extensive várzea forest as a barrier to terra firme birds [Poster presentation]. VII North American Ornithological Conference, online conference.

Naka, L. N., Bechtoldt, C. L., Magalli Pinto Henriques, L., & Brumfield, R. T. (2012). The role of physical barriers in the location of avian suture zones in the Guiana Shield, northern Amazonia. *American Naturalist*. https://doi.org/10.1086/664627

Naka, L. N., & Brumfield, R. T. (2018). The dual role of Amazonian rivers in the generation and maintenance of avian diversity. *Science Advances, 4*(8), eaar8575. https://doi.org/10.1126/sciadv.aar8575

Nuñez-Penichet, C., Cobos, M. E., Barro, A., & Soberón, J. (2019). Potential migratory routes of *Urania boisduvalii* (Lepidoptera: Uraniidae) among host plant populations. *Diversity and Distributions, 25*(3), 478–488. https://doi.org/10.1111/ddi.12881

Ödeen, A., & Håstad, O. (2013). The phylogenetic distribution of ultraviolet sensitivity in birds. *BMC Evolutionary Biology, 13*(1), 1–10. https://doi.org/10.1186/1471-2148-13-36

Oksanen, J., Blanchet, F. G., Kindt, R., Legendre, P., Minchin, P. R., O'hara, R. B., Simpson, G. L., Solymos, P., Stevens, M. H., Wagner, H., & Oksanen, M. J. (2013). Package 'vegan.' *Community Ecology Package, Version, 2*(9), 1–295.

Ortiz, D. A., Lima, A. P., & Werneck, F. P. (2018). Environmental transition zone and rivers shape intraspecific population structure and genetic diversity of an Amazonian rain forest tree frog. *Evolutionary Ecology, 32*(4), 359–378. https://doi.org/10.1007/s10682-018-9939-2

Osorio, D. (1996). Symmetry detection by categorization of spatial phase, a model. *Proceedings of the Royal Society B: Biological Sciences, 263*(1366), 105–110. https://doi.org/10.1098/rspb.1996.0017

Paradis, E., & Schliep, K. (2019). ape 5.0: An environment for modern phylogenetics and evolutionary analyses in R. *Bioinformatics, 35*(3), 526–528. https://doi.org/10.1093/bioinformatics/bty633

Patterson, N., Price, A. L., & Reich, D. (2006). Population structure and eigenanalysis. *PLoS Genetics, 2*(12), e190.

Pebesma, A. E., Bivand, R., & Pebesma, M. E. (2013). Package "sp" title classes and methods for spatial data. In *Citeseer*. https://r-forge.r-project.org/projects/rspatial/

Peterson, A. T. (1991). Gene flow in scrub jays: Frequency and direction of movement. *Condor, 93*(4), 926–934.

Peterson, A. T., Papeş, M., & Soberón, J. (2008). Rethinking receiver operating characteristic analysis applications in ecological niche modeling. *Ecological Modelling, 213*(1), 63–72. https://doi.org/10.1016/j.ecolmodel.2007.11.008

Phillips, S. J., Anderson, R. P., Dudík, M., Schapire, R. E., & Blair, M. E. (2017). Opening the black box: An open-source release of Maxent. *Ecography, 40*(7), 887–893. https://doi.org/10.1111/ecog.03049

Phillips, S. J., Anderson, R. P., & Schapire, R. E. (2006). Maximum entropy modeling of species geographic distributions. *Ecological Modelling, 190*(3–4), 231–259. https://doi.org/10.1016/j.ecolmodel.2005.03.026

Pirani, R. M., Werneck, F. P., Thomaz, A. T., Kenney, M. L., Sturaro, M. J., Ávila-Pires, T. C. S., Peloso, P. L. V., Rodrigues, M. T., & Knowles, L. L. (2019). Testing main Amazonian rivers as barriers across time and space within widespread taxa. *Journal of Biogeography*. https://doi.org/10.1111/jbi.13676

Prum, R. O. (2012). Aesthetic evolution by mate choice: Darwin's really dangerous idea. *Philosophical Transactions of the Royal Society B: Biological Sciences, 367*(1600), 2253–2265.

R Development Core Team. (2020). *R: A language and environment for statistical computing*. R Development Core Team.

Ramírez-Barrera, S. M., Velasco, J. A., Orozco-Téllez, T. M., Vázquez-López, A. M., & Hernández-Baños, B. E. (2019). What drives genetic and phenotypic divergence in the Red-crowned Ant tanager (*Habia rubica*, Aves: Cardinalidae), a polytypic species? *Ecology and Evolution, 9*(21), 12339–12352. https://doi.org/10.1002/ece3.5742

Reis, C. A., Dias, C., Araripe, J., Aleixo, A., Anciães, M., Sampaio, I., Schneider, H., & do Rêgo, P. S. (2020). Multilocus data of a manakin species reveal cryptic diversification moulded by vicariance. *Zoologica Scripta, 49*(2), 129–144. https://doi.org/10.1111/zsc.12395

Reynolds, R. G., & Fitzpatrick, B. M. (2007). Assortative mating in poison-dart frogs based on an ecologically important trait. *Evolution, 61*(9), 2253–2259. https://doi.org/10.1111/j.1558-5646.2007.00174.x

Ribas, C. C., Aleixo, A., Nogueira, A. C. R., Miyaki, C. Y., & Cracraft, J. (2012). A palaeobiogeographic model for biotic diversification within Amazonia over the past three million years. *Proceedings of the Royal Society B: Biological Sciences, 279*(1729), 681–689. https://doi.org/10.1098/rspb.2011.1120

Rojas, D., Lima, A. P., Momigliano, P., Simões, P. I., Dudaniec, R. Y., de Avila-Pires, T. C. S., Hoogmoed, M. S., da Cunha Bitar, Y. O., Kaefer, I. L., Amézquita, A., & Stow, A. (2020). The evolution of polymorphism in the warning coloration of the Amazonian poison frog *Adelphobates galactonotus*. *Heredity, 124*(3), 439–456. https://doi.org/10.1038/s41437-019-0281-4

Rosseel, Y. (2012). lavaan: An R package for structural equation modeling. *Journal of Statistical Software, 48*(2), 1–36. https://doi.org/10.18637/jss.v048.i02

Roulin, A., & Ducrest, A. L. (2013, June). Genetics of colouration in birds. In *Seminars in cell & developmental biology*. Academic Press.

Rull, V. (2011). Neotropical biodiversity: Timing and potential drivers. *Trends in Ecology and Evolution, 26*(10), 508–513. https://doi.org/10.1016/j.tree.2011.05.011

Rundle, H. D., & Nosil, P. (2005). Ecological speciation. *Ecology Letters, 8*(3), 336–352. https://doi.org/10.1111/j.1461-0248.2004.00715.x

Schietti, J., Martins, D., Emilio, T., Souza, P. F., Levis, C., Baccaro, F. B., da Veiga Pinto, J. L. P., Moulatlet, G. M., Stark, S. C., Sarmento, K., de Araújo, R. N. O., Costa, F. R. C., Schöngart, J., Quesada, C. A., Saleska, S. R., Tomasella, J., & Magnusson, W. E. (2016). Forest structure along a 600 km transect of natural disturbances and seasonality gradients in central-southern Amazonia. *Journal of Ecology, 104*(5), 1335–1346. https://doi.org/10.1111/1365-2745.12596

Schluter, D. (2001). Ecology and the origin of species. *Trends in Ecology and Evolution, 16*(7), 372–380. https://doi.org/10.1016/S0169-5347(01)02198-X

Seehausen, O., Terai, Y., Magalhaes, I. S., Carleton, K. L., Mrosso, H. D. J., Miyagi, R., Van Der Sluijs, I., Schneider, M. V., Maan, M. E., Tachida, H., Imai, H., & Okada, N. (2008). Speciation through sensory drive in cichlid fish. *Nature, 455*(7213), 620–626. https://doi.org/10.1038/nature07285

Servedio, M. R., & Boughman, J. W. (2017). The role of sexual selection in local adaptation and speciation. *Annual Review of Ecology, Evolution, and Systematics, 48*(July), 85–109. https://doi.org/10.1146/annurev-ecolsys-110316-022905

Sexton, J. P., Hangartner, S. B., & Hoffmann, A. A. (2014). Genetic isolation by environment or distance: Which pattern of gene flow is most common? *Evolution, 68*(1), 1–15.

Siddiqi, A., Cronin, T. W., Loew, E. R., Vorobyev, M., & Summers, K. (2004). Interspecific and intraspecific views of color signals in the strawberry poison frog *Dendrobates pumilio*. *Journal of Experimental Biology, 207*(14), 2471–2485. https://doi.org/10.1242/jeb.01047

Silva, S. M., Peterson, A. T., Carneiro, L., Burlamaqui, T. C. T., Ribas, C. C., Sousa-Neves, T., Miranda, L. S., Fernandes, A. M., d'Horta, F. M., Araújo-Silva, L. E., & Batista, R. (2019). A dynamic continental moisture gradient drove Amazonian bird diversification. *Science Advances, 5*(7), eaat5752. https://doi.org/10.1126/sciadv.aat5752

Simões, M., Romero-Alvarez, D., Nuñez-Penichet, C., Jiménez, L., & Cobos, M. E. (2020). General theory and good practices in ecological niche modeling: A basic guide. *Biodiversity Informatics, 15*(2), 67–68. https://doi.org/10.17161/bi.v15i2.13376

Simões, P. I., Stow, A., Hödl, W., Amézquita, A., Farias, I. P., & Lima, A. P. (2014). The value of including intraspecific measures of biodiversity in environmental impact surveys is highlighted by the Amazonian brilliant-thighed frog (*Allobates femoralis*). *Tropical Conservation Science, 7*(4), 811–828. https://doi.org/10.1177/194008291400700416

Smith, B. T., McCormack, J. E., Cuervo, A. M., Hickerson, M. J., Aleixo, A., Cadena, C. D., Pérez-Emán, J., Burney, C. W., Xie, X., Harvey, M. G., Faircloth, B. C., Glenn, T. C., Derryberry, E. P., Prejean, J., Fields, S., & Brumfield, R. T. (2014). The drivers of tropical speciation. *Nature, 515*(7527), 406–409. https://doi.org/10.1038/nature13687

Snow, D. (2020). Blue-crowned Manakin (*Lepidothrix coronata*), version 1.0. In J. del Hoyo, A. Elliott, J. Sargatal, D. A. Christie, & E. de Juana (Eds.), *Birds of the world.* Cornell Lab of Ornithology. https://doi.org/10.2173/bow.blcman1.01

Soberón, J., & Peterson, A. T. (2005). Interpretation of models of fundamental ecological niches and species' distributional areas. *Biodiversity Informatics, 2*, 1–10. https://doi.org/10.17161/bi.v2i0.4

Stabler, B., & Stabler, M. (2013). Package "shapefiles". http://www.lgc.com/resources/

Stephens, M., Smith, N. J., & Donnelly, P. (2001). A new statistical method for haplotype reconstruction from population data. *American Journal of Human Genetics, 68*(4), 978–989. https://doi.org/10.1086/319501

Stoddard, M. C., & Prum, R. O. (2008). Evolution of avian plumage color in a tetrahedral color space: A phylogenetic analysis of new world buntings. *American Naturalist, 171*(6), 755–776. https://doi.org/10.1086/587526

Summers, K., Symula, R., Clough, M., & Cronin, T. (1999). Visual mate choice in poison frogs. *Proceedings of the Royal Society B: Biological Sciences, 266*(1434), 2141–2145. https://doi.org/10.1098/rspb.1999.0900

Tajima, F. (1989). Statistical method for testing the neutral mutation hypothesis by DNA polymorphism. *Genetics, 123*(3), 585–595.

Tang, J., Hanage, W. P., Fraser, C., & Corander, J. (2009). Identifying currents in the gene pool for bacterial populations using an integrative approach. *PLoS Computational Biology, 5*(8), e1000455.

Teófilo, F. H. A., Schietti, J., & Anciães, M. (2018). Spatial and environmental correlates of intraspecific morphological variation in three species of passerine birds from the Purus-Madeira interfluvium, Central Amazonia. *Evolutionary Ecology, 32*(2–3), 191–214. https://doi.org/10.1007/s10682-018-9929-4

Thom, G., Do Amaral, F. R., Hickerson, M. J., Aleixo, A., Araujo-Silva, L. E., Ribas, C. C., Choueri, E., & Miyaki, C. Y. (2018). Phenotypic and genetic structure support gene flow generating gene tree discordances in an Amazonian floodplain endemic species. *Systematic Biology, 67*(4), 700–718. https://doi.org/10.1093/sysbio/syy004

Todd, W. E. C. (1925). Sixteen new birds from Brazil and Guiana. *Proceedings of the Biological Society Washington, 38*, 91–100.

van Etten, J. (2017). R package gdistance: Distances and routes on geographical grids. *Journal of Statistical Software, 76*, 1–21.

Vavrek, M. J. (2011). Fossil: Palaeoecological and palaeogeographical analysis tools. *Palaeontologia Electronica, 14*(1), 16.

Vermote, E., Justice, C., Claverie, M., & Franch, B. (2016). Preliminary analysis of the performance of the Landsat 8/OLI land surface reflectance product. *Remote Sensing of Environment, 185*, 46–56. https://doi.org/10.1016/j.rse.2016.04.008

Vorobyev, M., Brandt, R., Peitsch, D., Laughlin, S. B., & Menzel, R. (2001). Colour thresholds and receptor noise: Behaviour and physiology compared. *Vision Research, 41*(5), 639–653. https://doi.org/10.1016/S0042-6989(00)00288-1

Wang, I. J. (2013). Examining the full effects of landscape heterogeneity on spatial genetic variation: A multiple matrix regression approach for quantifying geographic and ecological isolation. *Evolution, 67*(12), 3403–3411. https://doi.org/10.1111/evo.12134

Wang, I. J., & Bradburd, G. S. (2014). Isolation by environment. *Molecular Ecology, 23*(23), 5649–5662. https://doi.org/10.1111/mec.12938

Wang, I. J., & Shaffer, H. B. (2008). Rapid color evolution in an aposematic species: A phylogenetic analysis of color variation in the strikingly polymorphic strawberry poison-dart frog. *Evolution, 62*(11), 2742–2759. https://doi.org/10.1111/j.1558-5646.2008.00507.x

Warren, D. L. (2012). In defense of "niche modeling." *Trends in Ecology and Evolution, 27*(9), 497–500. https://doi.org/10.1016/j.tree.2012.03.010

Warren, D. L., Glor, R. E., & Turelli, M. (2008). Environmental niche equivalency versus conservatism: Quantitative approaches to niche evolution. *Evolution, 62*(11), 2868–2883. https://doi.org/10.1111/j.1558-5646.2008.00482.x

Warren, D. L., & Seifert, S. N. (2011). Ecological niche modeling in Maxent: The importance of model complexity and the performance of model selection criteria. *Ecological Applications, 21*(2), 335–342. https://doi.org/10.1890/10-1171.1

Waterhouse, A. M., Procter, J. B., Martin, D. M. A., Clamp, M., & Barton, G. J. (2009). Jalview version 2—A multiple sequence alignment—JABAWS: MSA. *Bioinformatics, 27*, 1189–1191. https://doi.org/10.1093/bioinformatics/btp033

Weir, J. T., & Schluter, D. (2008). Calibrating the avian molecular clock. *Molecular Ecology, 17*(10), 2321–2328. https://doi.org/10.1111/j.1365-294X.2008.03742.x

Werle, E., Schneider, C., Renner, M., Vöker, M., & Fiehn, W. (1994). Convenient single-step, one tube purification of PCR products for direct sequencing. *Nucleic Acids Research, 22*(20), 4354.

Wright, S. (1943). Isolation by distance. *Genetics, 28*(2), 114–138.

Zeh, J. A., Zeh, D. W., & Bonilla, M. M. (2003). Phylogeography of the harlequin beetle-riding pseudoscorpion and the rise of the Isthmus of Panamá. *Molecular Ecology, 12*(10), 2759–2769. https://doi.org/10.1046/j.1365-294X.2003.01914.x

Zimmer, J. T. (1936). Studies of Peruvian birds. No XXII. Notes on the Pipridae. *American Museum Novitates, 893*, 1–29.

Authors and Affiliations

Pedro Paulo[1,2] · Fernando Henrique Teófilo[1,2,14] · Carolina Bertuol[1,3,12] · Érico Polo[3] · Andre E. Moncrieff[4] · Lucas N. Bandeira[1,2] · Claudia Nuñez-Penichet[5] · Igor Yuri Fernandes[2] · Mariane Bosholn[1,2,6] · Arielli F. Machado[1,7] · Leilton Willians Luna[9,10] · Willian Thomaz Peçanha[8] · Aline Pessutti Rampini[1,2] · Shizuka Hashimoto[1,3] · Cleyssian Dias[9,10] · Juliana Araripe[9] · Alexandre Aleixo[10,11,15] · Péricles Sena do Rêgo[9] · Tomas Hrbek[3,12] · Izeni P. Farias[3,12] · A. Townsend Peterson[5] · Igor L. Kaefer[2,13] · Marina Anciães[1,2]

✉ Pedro Paulo
pedropaulofers@gmail.com

1 Laboratório de Evolução e Comportamento Animal – LABECA, Coordenação de Biodiversidade – COBIO, Instituto Nacional de Pesquisas da Amazônia, Campus III, Av. André Araújo, 2936, Manaus, Amazonas CEP: 69067-375, Brazil

2 Programa de Pós-Graduação em Ecologia, Instituto Nacional de Pesquisas da Amazônia, Campus III, Av. André Araújo, 2936, Manaus, Amazonas CEP: 69067-375, Brazil

3 Laboratório de Genética e Evolução Animal – LEGAL, Instituto de Ciências Biológicas, Departamento de Genética, Universidade Federal do Amazonas, Av. Rodrigo Otávio, 6200, Manaus, Amazonas CEP: 69080-900, Brazil

4 Department of Biological Sciences and Museum of Natural Science, Louisiana State University, Baton Rouge, LA, USA

5 Department of Ecology and Evolutionary Biology and Biodiversity Institute, University of Kansas, 1345, Jayhawk Boulevard, Lawrence, KS 66045, USA

6 Centro de Estudos em Biodiversidade (CBio), Universidade Federal de Roraima (UFRR), Avenida Capitão Enê Garcês, Boa Vista, Roraima CEP: 69310-000, Brazil

7 Laboratório de Ecologia e Filogenética Funcional – LEFF, Universidade Federal do Rio Grande do Sul (UFRGS), Avenida Bento Gonçalves, 9500, 43113, Porto Alegre, Rio Grande do Sul CEP: 91501-970, Brazil

8 Laboratório de Citogenética e Evolução – LACE, Programa de Pós-graduação em Genética e Biologia Molecular, Departamento de Genética, Universidade Federal do Rio Grande do Sul (UFRGS), Av. Bento Gonçalves, 9500, 43312, Porto Alegre, Rio Grande do Sul CEP: 91501-970, Brazil

9 Laboratório de Genética e Conservação, Instituto de Estudos Costeiros, Universidade Federal do Pará, Campus Universitário de Bragança, Alameda Leandro Ribeiro, S/N, Bragança, Pará CEP: 68600-000, Brazil

10 Programa de Pós-Graduação em Zoologia, Universidade Federal do Pará, Museu Paraense Emílio Goeldi, Belém, Pará, Brazil

11 Finnish Museum of Natural History, University of Helsinki, Helsinki, Finland

12 Programa de Pós-Graduação em Genética, Conservação e Biologia Evolutiva, Instituto Nacional de Pesquisas da Amazônia, Campus II, Av. André Araújo, 2936, Manaus, Amazonas CEP: 69067-375, Brazil

13 Departamento de Biologia, Universidade Federal do Amazonas, Av. Rodrigo Otávio, 6200, Manaus, Amazonas CEP: 69080-900, Brazil

14 Instituto Federal de Educação, Ciência e Tecnologia do Amazonas, Campus Tefé, Tefé, Amazonas, Brazil

15 Instituto Tecnológico Vale - ITV, Rua Boaventura da Silva, 955, Belém CEP: 66055-090, Brazil